Successful Completion of SIM-PlanetQuest Technology

Robert A. Laskin[1]
Jet Propulsion Laboratory, California Institute of Technology

ABSTRACT

Optical interferometry will open new vistas for astronomy over the next decade. The Space Interferometry Mission (SIM-PlanetQuest), operating unfettered by the Earth's atmosphere, will offer unprecedented astrometric precision that promises the discovery of Earth-class extra-solar planets as well as a wealth of important astrophysics. Optical interferometers also present severe technological challenges: laser metrology systems must perform with sub-nanometer precision; mechanical vibrations must be controlled to nanometers requiring orders of magnitude disturbance rejection; a multitude of actuators and sensors must operate flawlessly and in concert. The Jet Propulsion Laboratory, with the support of Lockheed Martin Advanced Technology Center (LM ATC) and Northrop Grumman Space Technology (NGST), has addressed these challenges with a technology development program that is now complete. Technology transfer to the SIM flight team is now well along and the project is proceeding toward Preliminary Design Review (PDR) with a quickening pace.

Keywords: interferometry, metrology, pointing, control, nanometer, picometer, optics, lasers

1. INTRODUCTION

SIM-PlanetQuest, with a target launch date early in the next decade (budget permitting), will be one of the premiere missions in NASA's astronomy and astrophysics program. SIM's niche is to detect planets around stars in our neighborhood of the Milky Way galaxy. SIM aims to find solar systems like our own and will be sensitive enough to identify Earth-like planets in these solar systems. This adventure of discovery will be enabled by an explosive growth of innovative technology, as exciting in its own right as the underlying scientific quest. SIM-PlanetQuest (see Fig. 1) drives the state-of-the-art in optomechanical and optoelectronic systems as well as presenting daunting challenges in precise stabilization of lightweight deployable structures and coordinated computer control of numerous optical surfaces.

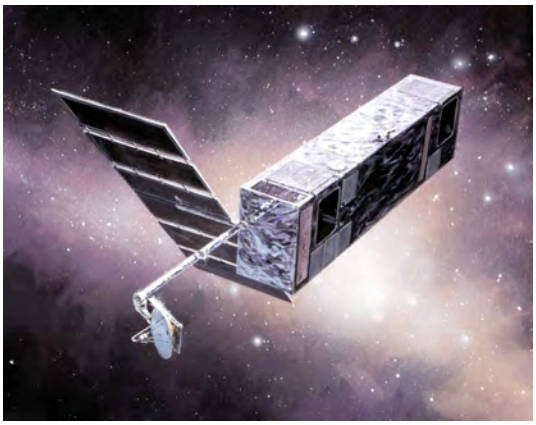

Fig. 1: Artistic conception of SIM.

Fig. 2 shows the layout of the SIM instrument, which occupies most of the volume within the flight system depicted in Fig. 1. The instrument consists of three individual optical interferometers whose baselines are parallel. Each baseline is approximately 9 meters long, implying that SIM will be a large payload filling the entire shroud of an expendable launch vehicle of the Delta IV or Atlas V class. The mission design calls for SIM to be placed in an Earth-trailing orbit similar to that of the Spitzer Space Telescope. Such an orbit has the system orbiting the Sun at 1 AU but falling increasingly behind the orbit of Earth as the mission proceeds. This will provide an extremely stable thermal environment for the instrument while maintaining sufficient communication rates. Each of SIM's three interferometers consists of two 33-cm aperture telescopes that compress the starlight beams down to about 3.5 cm and route the light through beam trains to the beam combiner where stellar interference fringes are formed. The telescopes of the two guide interferometers are pointed directly at guide stars, which are used to provide precise inertial reference for the instrument. The telescopes of the science interferometer are fixed to the precision structure, but each one has a steering flat in front of it, which can pick

[1] robert.a.laskin@jpl.nasa.gov; phone 1 818 354-5086; fax 1 818 393-5239; http://www.jpl.nasa.gov/sim; Jet Propulsion Laboratory, 4800 Oak Grove Drive, Pasadena, CA, USA 91109-8099

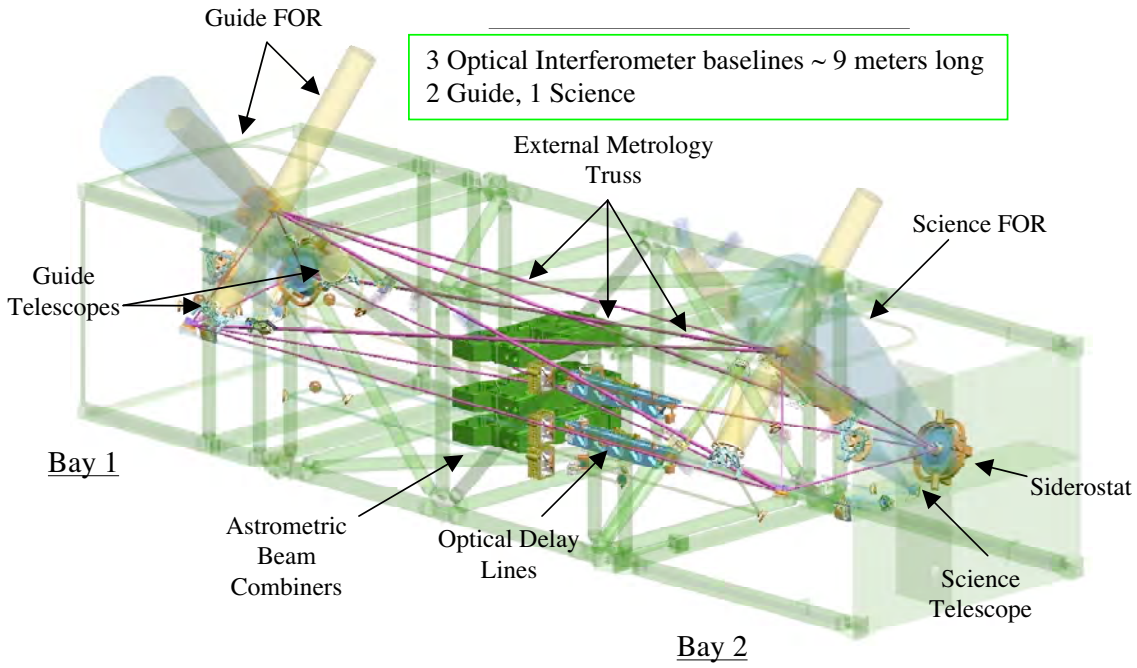

Fig. 2 SIM Interferometer Instrument

out stars over a 15-degree conical field of regard (FOR). These steering flats are called "siderostats." The guide telescopes and science telescopes along with the science siderostats are packaged together at each end of the structure in "Bays" 1 and 2. The guide telescopes and science siderostats are optically connected to one another by an "external metrology truss" whose 14 laser beams query corner cubes located in the centers of the siderostats and immediately in front of the guide telescopes. This allows the external metrology to determine the relative orientation of the interferometer baselines to sub-nanometer precision.

2. MAJOR TECHNICAL CHALLENGES

This paper proceeds by discussing the key technical challenges faced by SIM and the technology development approach to meet them. As an overview paper, there is appended an extensive list of references which contain greater technical detail on the various elements of interferometry technology. A short digression on how SIM makes astrometry measurements is necessary to motivate the enabling technology.

Let's start by considering a simplified layout of a single generic interferometer depicted in Fig. 3. Think of this as SIM's science interferometer and ignore the fact that telescopes are shown as directly receiving the starlight rather than siderostats. Starlight from a "Star A" is collected by both "telescope 1" and "telescope 2" and is combined at the interferometer's "beam combiner" where a fringe pattern is imaged on the "detector." A fringe pattern will appear on the detector only if the total distance traversed by stellar photons from the star through each arm of the interferometer is equal (to within a few microns). In order to equalize the stellar pathlengths, the "delay line" must be positioned such that an amount of "internal path delay" is added to arm 2 of the interferometer to offset the "external path delay" experienced by arm 1. Now imagine that the interferometer baseline "B" is sitting absolutely still in inertial space. In order to measure the angle, θ, between Star A and another star (call it Star B), the interferometer's telescopes are slewed from Star A to acquire Star B and the delay line is repositioned by a distance "d" (called the differential delay) such that the

stellar fringe for Star B appears on the detector. Now the angle θ can be determined by measuring the differential delay and, to first order, dividing it by the baseline length B. How do we measure the differential delay? We do so with a laser metrology gauge that constantly samples changes in the path lengths internal to the interferometer by launching laser beams from the beam combiner through both arms of the interferometer out to corner cubes in front of the two telescopes (or on the siderostats, as the case may be). The beams return from the corner cubes and, having hit all optical surfaces internal to the interferometer, allow the "internal" metrology gauge to monitor the differential delay. So, an interferometer does astrometry by measuring the differential delays between a field of stars. By observing star field after star field, the positions of stars over the entire sky can be mapped. The accuracy of the star map is directly proportional to the accuracy of the differential delay measurements. SIM, for its planet finding science, aims to measure angles between stars to an accuracy of 1 microarcsecond (5 picoradians). Hence, the requirement on internal metrology is to measure differential delays to order of 50 picometers. Two additional requirements emerge by reference to Fig. 3: (i) the position of the stellar fringe on the detector must also be read out to an accuracy of order 50 picometers; (ii) the stellar fringe must be stable on the detector at about the 10-nanometer level in order to provide a crisp "high visibility" fringe that can be read with the accuracy just mentioned.

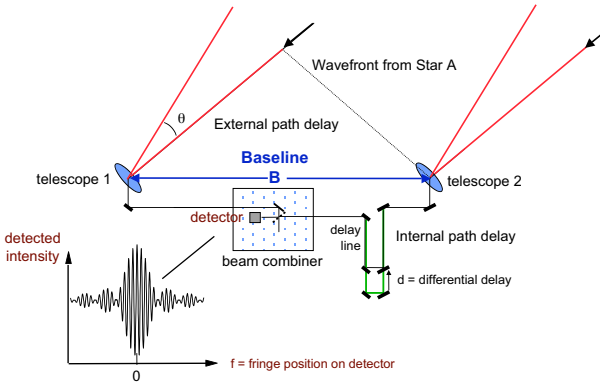

Fig. 3: Measuring the angle between two stars.

One problem left to be resolved from the discussion above is the assumption that the science interferometer baseline B is sitting absolutely still in inertial space. In reality, it will be moving at the level that the attitude control system (ACS) of the spacecraft allows. SIM will use an ACS that will control the interferometer to a stability of about 0.1 arcsecond, almost one million times larger than the star angle error requirement. So, we will need a means of providing knowledge of the attitude of the science baseline at the microarcsecond level as it wanders around. This knowledge is provided by SIM's two "guide interferometers" working in concert with the "external metrology" truss (see Fig. 4). The figure shows six corner cubes (the spherical balls that delineate a roughly 9m x 2m x 2m triangular prism) connected pair-wise by 14 metrology beams forming the external metrology truss. Each of the 14 legs of the external metrology truss consists of a metrology gauge very similar to the internal metrology gauge described above. The two corner cubes at the top of the figure sit in front of the four telescopes that comprise the two guide interferometers. Another way of saying this is the two guide interferometers share a common baseline called out as the "guide baseline" in the figure. The "science baseline" is shown in the foreground of the figure and is delineated by the two corner cubes that sit on the science siderostats. The attitude motion of the science baseline is tracked as follows: (i) the guide interferometers track the motion of the guide baseline by maintaining lock on bright guide star stellar fringes while monitoring the guide interferometer internal metrology gauges; (ii) the external metrology truss transfers the attitude of the guide baseline to the science baseline. All of this, of course, needs to be done with microarcsecond precision, leading

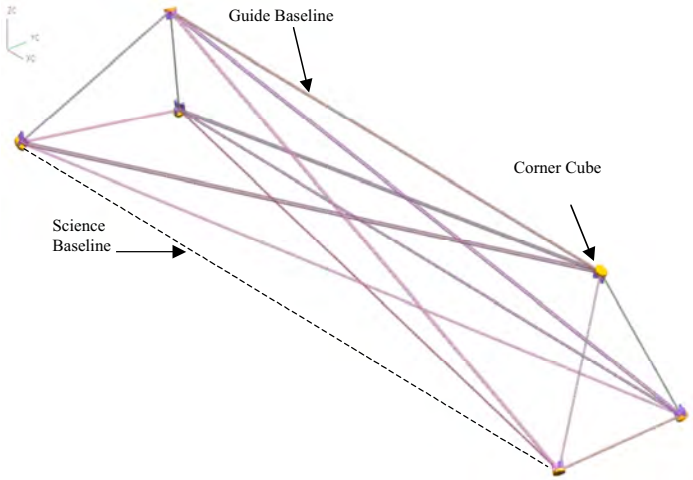

Fig 4: Maintaining microarsecond knowledge of the motion of the science baseline

to the requirement that the metrology gauges of the external metrology truss make measurements with picometer regime errors, similar to the requirements on the internal metrology gauges.

Hence, successful development of SIM requires that two grand technological challenges be met and overcome:

(1) picometer level sensing of stellar fringe position and optical element relative positions over meters of separation distance
(2) nanometer level control and stabilization of optical elements on a lightweight flexible structure

A third significant technical challenge has to do with overall instrument complexity and the implications for interferometer integration and test. SIM is representative of an emerging class of large optical instruments that are not fully testable, in an end-to-end fashion, prior to launch. SIM will need to be tested in two or three major "chunks" which, to first order, are independent of one another. SIM's end-to-end instrument performance is then knitted together from a combination of chunk-level test results and high fidelity analytical models. Thus, SIM challenges engineers and managers to work together in arriving at an approach to instrument integration and test, which is simultaneously feasible, effective in maximally reducing risk, and affordable. SIM also places a premium on models since they will be such a fundamental part of instrument validation and verification. SIM's reliance on analytical models for system "buy-off" is not unprecedented but is certainly well beyond the norm.

3. TECHNOLOGY DEVELOPMENT

Fundamentally, the approach taken to technology development was one of rapid prototyping of critical hardware and software followed by integration into technology testbeds where critical interfaces could be validated, system level performance demonstrated, integration and test procedures developed and verified, and analytical modeling methods validated. This approach placed the ground testbeds at the very heart of the technology development effort. It was in these testbeds that the technology products were validated and technology readiness demonstrated. It was also in these testbeds that our engineering team learned about what works and what does not when it comes to integrating and testing interferometers.

Given the size of the technological challenges presented by SIM and the, accordingly large resources devoted to their solution, a high degree of programmatic rigor was imposed on the technology development program. A formal Technology Plan was released in April 2003 at the time of the project's Preliminary Mission and Systems Review. The Technology Plan contained eight major milestones, dubbed Technology Gates, that the technology program committed to complete in order to demonstrate readiness to proceed into flight system implementation. These Technology Gates, originally contained in a May 2001 letter from NASA Headquarters to JPL, were consistent with progressing from NASA's Technology Readiness Level (TRL) 4, "component and/or breadboard validation in laboratory environment," through TRL 6, "system/subsystem model or prototype demonstration in a relevant environment (ground or space)."
The Technology Gates are stated below in synoptic form. References are made to technology testbeds and components that are described below.

Technology Gate 1: Next generation metrology beam launcher performance at 100pm uncompensated cyclic error, 20 pm/mK thermal sensitivity.

Technology Gate 2: Achieve 50dB fringe motion attenuation on the SIM System Testbed (STB-3) demonstrating science star tracking.

Technology Gate 3: Demonstrate Micro-arcsecond Metrology (MAM) Testbed performance of 150pm over its narrow angle field of regard.

Technology Gate 4: Demonstrate Kite Testbed performance at 50pm narrow angle, 300pm wide angle.

Technology Gate 5: Demonstrate MAM Testbed performance at 4000pm wide angle.

Technology Gate 6: Benchmark MAM Testbed performance against narrow angle goal of 24pm.

Technology Gate 7: Benchmark MAM Testbed performance against wide angle goal of 280pm.

Technology Gate 8: Demonstrate SIM instrument performance via testbed anchored predicts against science requirements.

The Technology Gates were not intended to be comprehensive. Rather, they were important way stations used by NASA to track the project's technology progress. Gate 1 represented the completion of the necessary technology components, which advanced readiness to TRL 4/5 (TRL 5 = "component and/or breadboard validation in relevant environment"). Gate 2 represented demonstration of the necessary level of vibration control in a system setting, achieving TRL 6 for the nanometer stabilization technologies. Gates 3-7 demonstrated the picometer sensing technologies in subsystem testbeds representative of SIM's external metrology truss (Kite Testbed) and SIM's science interferometer (MAM Testbed), bringing these technologies to TRL 6.

Technology Gate 8 held a special place in the program. Its aim was to demonstrate readiness to integrate and test an instrument of SIM's scope and complexity. In two ways, Gate 8 represented a "dry run" for instrument integration and test. Firstly, each of the testbeds contributing data to the Gate 8 metric was a rehearsal of a specific future test set to be run on the flight instrument or a subsystem of the flight instrument. Secondly, the all-up integrated model of instrument performance, into which the testbed data was fed, is the same model that will be used to process future flight instrument test data and produce performance predictions against which flight system launch readiness decisions will be made.

Technology Gate	Description	Due Date	Complete Date	Performance
1	Next generation metrology beam launcher performance at 100pm uncompensated cyclic error, 20pm/mK thermal sensitivity	8/01	8/01	Exceeded objective
2	Achieve 50dB fringe motion attenuation on STB-3 testbed (demonstrates science star tracking)	12/01	11/01	Exceeded objective
3	Demonstrate MAM Testbed performance of 150pm over its narrow angle field of regard	7/02	9/02	Exceeded objective
4	Demonstrate Kite Testbed performance at 50pm narrow angle, 300pm wide angle	7/02	10/02	Exceeded objectives
5	Demonstrate MAM Testbed performance at 4000pm wide angle	2/03	3/03	Exceeded objective
6	Benchmark MAM Testbed performance against narrow angle goal of 24pm	8/03	9/03	Exceeded objective
7	Benchmark MAM Testbed performance against wide angle goal of 280pm	2/04, 5/04*	6/04	Met objective
8	Demonstrate SIM instrument performance via testbed anchored predicts against science requirements	4/05	7/05	Met objective

Legend
pm = picometer
mK = milliKelvin
dB = decibel (50dB = factor of 300)

* HQS directed a scope increase (by adding a numerical goal to what had been a benchmark Gate) and provided a 3 month extension when performance fell short

Table 1: Accomplishment of Technology Gates against original due dates stated in May 2001 letter

The technology program's ability to accomplish the Technology Gates is depicted in Table 1. Passage of each Gate was contingent upon a rigorous review process conducted by two review boards: the project appointed SIM Technical Advisory Committee (SIMTAC) and the NASA-appointed External Independent Review Board (EIRB). The remainder of this paper is devoted to a moderately detailed overview of the technology development achievements behind the Technology Gates. The reader is referred to the extensive bibliography at the end of the paper for greater insight into particular aspects of the technology effort.

3.1 Component Hardware Development

Breadboards and brassboards of the new technology components required by SIM were built and tested by the technology program. The objectives were threefold: mitigate technical, schedule, and cost risk associated with key hardware components early in the SIM project life cycle (when the cost of correcting problems is low); deliver necessary components to the technology integration testbeds; transition the capability to manufacture the components to the flight team.

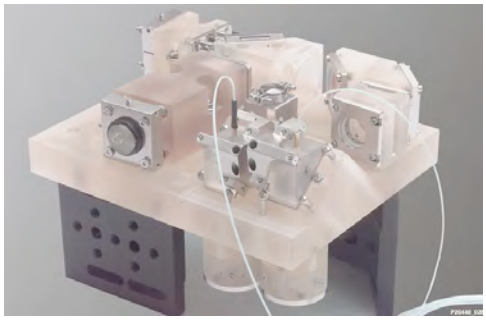

Fig. 5: Photo of breadboard metrology beam launcher built by Lockheed Martin

Several years ago, the project completed demonstrations of all the key pieces of component

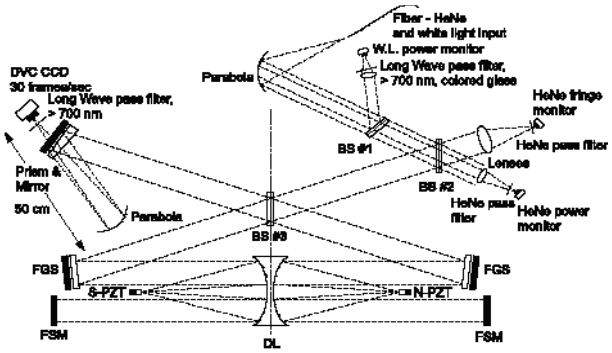

Fig 6 : Layout of white light fringe detection experiment.

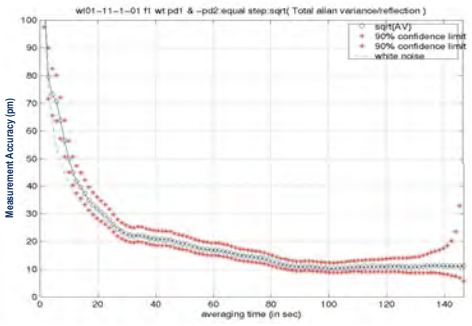

Fig. 7: Allan variance of consistency between white light fringe readout and He-Ne laser gauge.

technology. The most critical of these were laser metrology, with relative motion accuracies less than 50 pm, and white light fringe sensors with less than 30 pm error. A laser metrology gauge consists of a beam launcher interposed between two corner cubes whose relative motion is to be measured. The beam launcher has a detector capable of sensing minute changes in the phase of the laser beam that interrogates the two corner cubes. Fig. 5 shows a photo of a breadboard beam launcher built by LM ATC in 2001. It was built mostly out of zerodur parts since thermal stability is very important. Test data taken in August 2001 established that we succeeded in building a laser gauge with less than 100 pm of error over microns of corner cube motion and with thermal stability of less than 8 pm/mK of bulk temperature change, satisfying Technology Gate 1. Performance against both of these parameters has since been significantly improved with the fabrication of brassboard beam launchers.

The "white light experiment," conducted in December 2001, demonstrated the ability to measure broadband "stellar" fringe positions to less than 30 pm. Fig. 6 shows a layout of the white light experiment. White light was fed into the beam combiner, propagated backward through the beam combiner and delay line and was retro-reflected by the fast steering mirror back to the CCD camera fringe detector. Fringe estimates were made by monitoring the fringe intensity pattern while modulating the optical path approximately one wave using the PZT stage of the delay line. A He-Ne laser was simultaneously injected into the white light fiber and was used as a truth reference for the fringe position. Fig. 7 shows an Allan Variance curve (bounded by 90% confidence error bar curves) of the difference between the phase estimate from the white light fringe detector and the He-Ne laser signal. At the 30 second integration time planned for SIM, fringe read error was about 22 pm, beating the flight requirement with margin. This was a huge step forward for the SIM technology development effort.

As a means of technology transfer, the flight team has collaborated with the technologists to build and test several of the higher risk components as brassboards (near flight form, fit, and function). In addition to the metrology beam launchers mentioned above, brassboards of the collector telescope, siderostat steering flat, double corner cube optical fiducial, and portions of the laser metrology source have been built. Figures 8, 9 and 10 show photographs of the collector telescope, siderostat steering flat, and double corner cube, respectively.

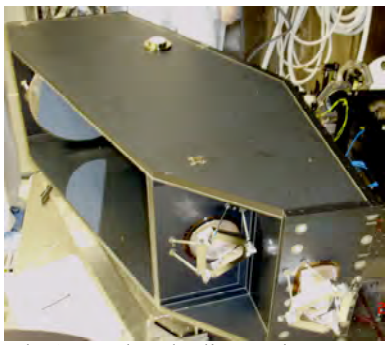

Fig. 8: Brassboard collector telescope

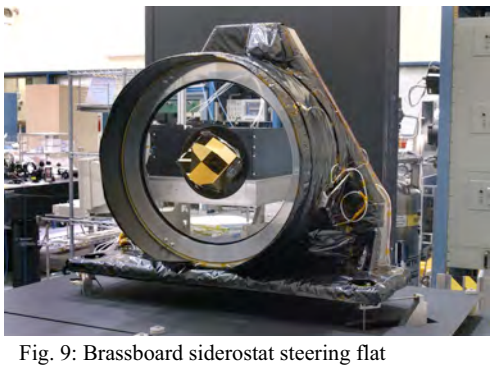

Fig. 9: Brassboard siderostat steering flat

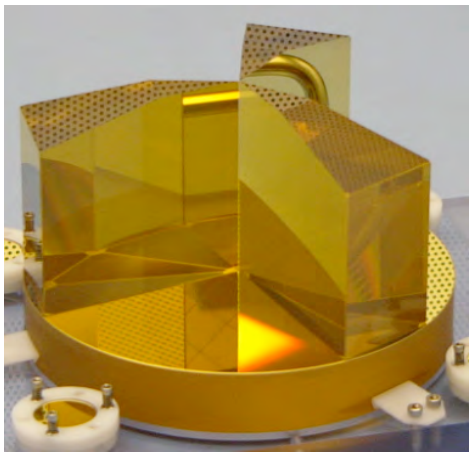

Fig. 10: Brassboard double corner cube

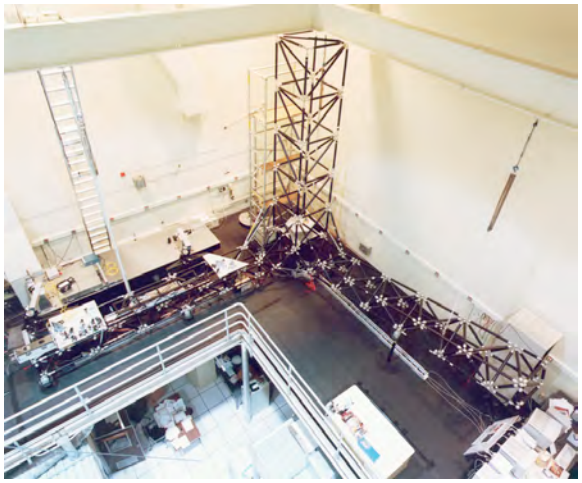

Fig. 11: Bird's eye view of STB-1.

3.2 Ground Integration Testbeds

At the outset of the technology development effort, optical interferometry was not yet sufficiently mature to allow us to assure system performance on the basis of an exhaustive set of component tests. Rather, it was necessary to do validation testing at higher levels of integration to prove that the technology played together. NASA requires a technology readiness level of 6, defined as "system/subsystem model or prototype demonstration in a relevant environment (ground or space)" in order for a project to proceed to flight implementation. For SIM, this was accomplished in the ground testbeds.

Four major ground testbeds were built and have completed their technology demonstration objectives: the evolutionary SIM System Testbed (STB-1,3), the Microarcsecond Metrology (MAM) Testbed, the Kite Testbed, and the Thermal Optomechanical (TOM) Testbed. This particular delineation of the ground testbed effort derived primarily from the desire that the technology testbeds closely resembled major instrument systems or subsystems. Thus, STB was built to emulate the instrument's structure and stabilization systems, MAM was constructed to simulate the sensing functions of the 3 interferometers, and Kite was built in the image of the external metrology truss. By representing each of the major instrument systems with a testbed, completeness of the technology effort was also insured.

Of equal importance to the testbeds' hardware demonstration function was their use as platforms for validating a broad class of modeling methods and techniques. Optical codes, especially for diffraction models, were validated on MAM and Kite. Millikelvin thermal codes and picometer distortion optomechanical codes were validated on TOM. Nanometer regime structural dynamics codes were validated on STB. Since SIM relies so heavily on modeling to inform flight system requirements derivation design, as well as integration and test, the legacy of validated models is perhaps the technology program's greatest long term contribution. The modeling team worked closely with each testbed team to build testbed models. These models typically achieved agreement with testbed data within a factor of two. Correlation between model and test allowed the calculation of modeling uncertainty factors (or MUF's). MUF's are already in use in the flight design where they are applied to flight model predictions to produce suitably conservative estimates of flight performance. On many occasions, the modelers were also key to diagnosing hardware problems encountered in the testbeds. In the testbed descriptions below modeling results will be interspersed on a testbed by testbed basis.

SIM System Testbed (STB)—The SIM System Testbed was actually an evolutionary series of two testbeds. The first, STB-1, was built during the 1991 through 1994 timeframe. It was a full single baseline interferometer built on a flexible structure (see Fig. 11) out of breadboard hardware components. The structure was a 7m × 6.8m × 5.5m aluminum truss weighing 200 kg (with optics and control systems attached with the weight at about 600 kg). Three active gravity off-load devices made up the structure's suspension system providing about a factor of ten separation between the structure's "rigid body" and flexible body modes (the lowest of which was at about 6 Hz). The equipment complement included a three tier optical delay line with associated laser metrology, a pointing system complete with two gimballed siderostats,

two fast steering mirrors, and coarse and fine angle tracking detectors, a six-axis isolation system, and all associated electronics and real time computer control hardware necessary for closed loop system control and data acquisition. The principal objectives of STB-1 were demonstrating vibration attenuation technologies and validating modeling tools in the nanometer regime. STB-1 was completed during the summer of 1994 when "first fringes" were acquired. Two metrics were tracked over time to monitor testbed progress. These were: (a) pseudo-star fringe tracking stability in the presence of the laboratory ambient vibration environment and; (b) fringe stability vs. emulated spacecraft reaction wheel disturbances, which are expected to be the dominant on-orbit disturbance source. Better than 5 nm RMS performance was achieved for each metric.

Experiments were conducted utilizing both a flight spare reaction wheel as the disturbance source as well as a laboratory

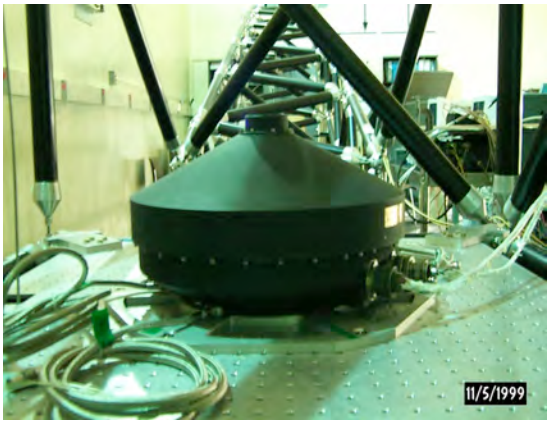

Fig. 12: Flight spare Magellan reaction wheel hard mounted on STB-1

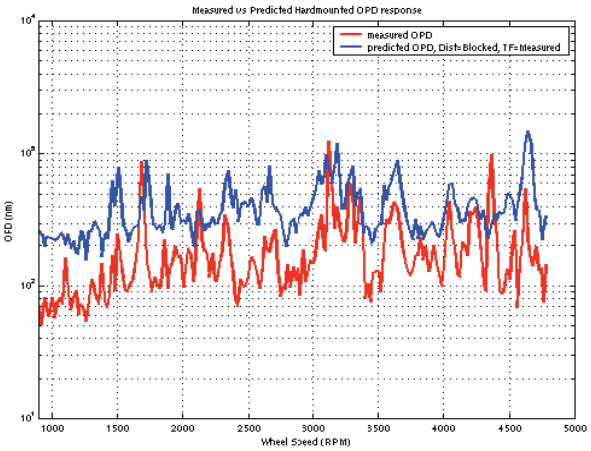

Fig. 13: Wheel response; predict vs measurement.

shaker. Fig. 12 shows the wheel mounted on the structure. The motivation was to verify that we could accurately predict the response to an actual wheel, which, with its internal compliance and mass distribution, is a more complex mechanical device than a shaker. Fig. 13 shows a comparison between the predicted response (darker trace) with the measured response (lighter trace) as a function of wheel speed. Notice that the prediction nicely over bounds the measurement by about a factor of two at most wheel speeds, lending confidence that our predictive capabilities are both accurate and conservative. Note also that the high levels of response (hundreds of nanometers) are due to the facts that (i) the wheel is much noisier than the ones intended for use on SIM, and (ii) the data was taken with the wheel in the hard mounted configuration.

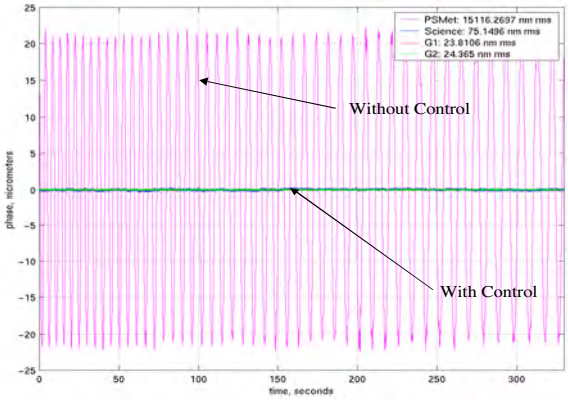

Fig. 14: Time domain dim star tracking data.

As the name implies, STB-3 is a three-baseline testbed. Its objectives were twofold: (1) to demonstrate in a realistic vibration environment that information from the guide interferometers and the metrology system can be fed at high bandwidth to the science interferometer enabling it to track, in angle and phase, dim science stars; (2) to demonstrate the capability to integrate and operate a system of comparable complexity to the flight instrument, thereby serving as a pathfinder for the flight system integration and test. The STB-3 approach has been to proceed in two phases. In Phase 1, we developed dim star phase tracking on optical tables, which entailed three-baseline "pathlength feedforward." Phase 2 moved the three interferometers onto a SIM-scale flexible structure and repeated the dim star tracking experiments, demonstrating rejection of disturbances in a flight traceable configuration.

Phase 1 testing on optical tables was completed in late 2001 and satisfied Technology Gate 2. We tracked fringes on all three interferometers and stabilized dim star fringes at flight levels in the face of simulated spacecraft attitude motions of the table. Figs. 14 and 15 show, respectively in the time and frequency domains, the level of attenuation achieved. The 80 dB rejection represents a factor of 10,000 and easily meets the level of performance required of the flight system.

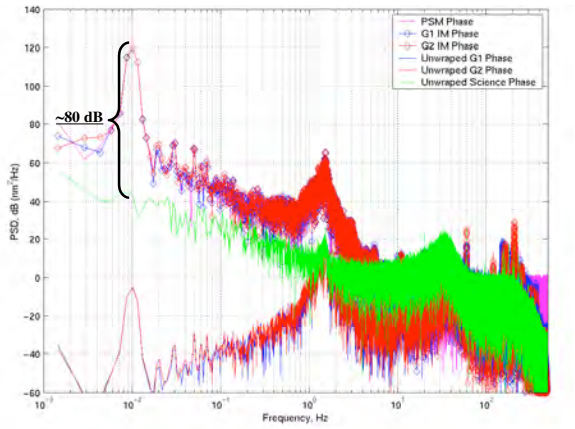

Fig. 15: Frequency domain dim star tracking data.

For Phase 2, all the optics were moved onto the 9-meter flexible structure pictured in Fig. 16 (with the optical bench for the pseudostar shown in the foreground). The structure was manufactured at NGST with emphasis on trying to mimic the dynamical characteristics of the flight precision structure for which NGST is also responsible. The CAD drawing of Fig. 17 gives a good idea of what the overall layout looks like with the optics in place. Also indicated in the figure are the laser metrology beams that tie the 3 baselines together. A full 15 laser beam external metrology system is operational on the testbed and has been functioning flawlessly now for over two years. Fringe tracking has been implemented on all three interferometers with performance in the face of lab ambient disturbances at or exceeding that achieved during Phase 1 or on STB-1 (see Fig. 18). This is largely due to the quietness of the new lab in which the testbed is now located.

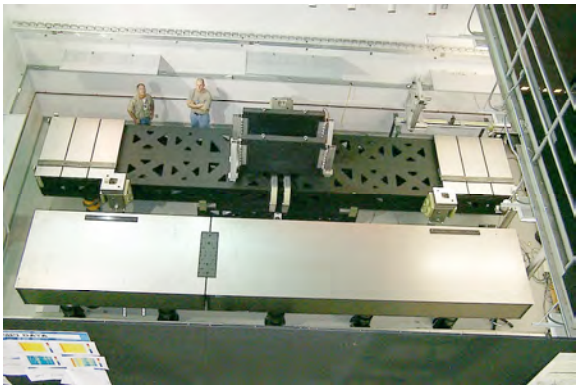
Fig. 16: STB-3 structure (shown upper portion of photo) installed in laboratory high bay

Perhaps the most important work done on STB-3 were experiments performed to validate the project's analytical modeling approach for predicting the flight system's dynamics. NGST modeling personnel produced a high fidelity finite element model (FEM) of the STB-3 structure along with all the optical elements and vibration isolation hardware (the STB-3 isolators were also manufactured by NGST). The modeling tools employed and granularity of the FEM mesh were identical to those that NGST typically employs in the modeling of flight systems. Analytical transfer functions were generated to predict the response of science interferometer optical path difference (i.e., "stellar" fringe motion) to mechanical disturbances arising in the "back-pack" portion of the testbed, which is slung below and vibration-isolated from the precision structure (see Fig. 17). The "back-pack" was built to be representative of a spacecraft equipment bay that would contain vibration sources such as reaction wheels for vehicle attitude control. Figure 19 shows the analytical transfer function compared to the same transfer function measured in the laboratory on the testbed. Clearly, the agreement is striking. When frequency-binned portions of these transfer functions are quantitatively compared, the data in Figure 20 results. The ratio of model prediction RMS energy to test data RMS energy never differs by more than a factor of two for any frequency bin or any axis of excitation. Most of the ratios are quite a bit smaller than factor of two. We conclude that the adoption of a modeling uncertainty factor (MUF) of two for

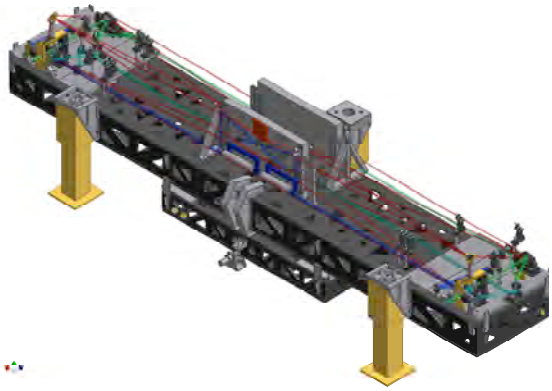
Fig. 17: CAD drawing of STB-3 with optics and metrology on 9-meter flexible structure.

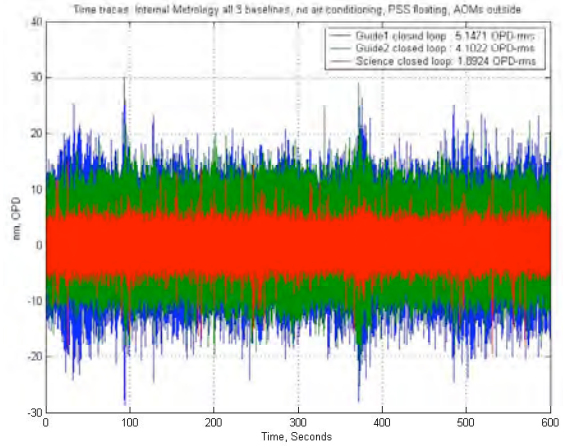

Fig. 18: "Stellar" fringe tracking performance on each of

this class of models would be conservative. Hence, as the design of the SIM flight system matures, a MUF of at leas two will be applied to flight transfer function predictions to insure that adequate margin for disturbance transmission is maintained.

Microarcsecond Metrology (MAM) Testbed—MAM is a single baseline white light interferometer fed by a reverse interferometer pseudostar (see Fig. 21) and was operational at JPL from early 2002 until April 2006. The testbed objective was to demonstrate that the stellar interferometers that comprise the SIM instrument are capable of making 1 microarcsecond differential angular measurements through the use of laser metrology and stellar fringe positional measurements. This being perhaps the most fundamental demonstration of the technology program, four of the eight Technology Gates were assigned to MAM.

MAM's single interferometer included siderostats for wide-angle acquisition, fast steering mirrors for high precision pointing, a delay line to control optical path and a beam combiner with both pointing and pathlength sensors. Additionally, internal metrology beams integrated into the beam combiner were used to measure the optical path between the combiner and each arm of the interferometer. An inverse interferometer pseudostar (IIPS), provided by LM ATC, was used to feed white light into the MAM interferometer (see photo in Fig. 22). The IIPS also used internal metrology beams that monitor the optical path from its main beamsplitter to the fiducials on the MAM interferometer. By comparing the white light fringe measurement and the metrology measurements from both the interferometer and the pseudostar as the angle of the "star" is varied, one could measure optical path measurement errors arising from a number of sources that are present on SIM. These include diffraction effects from moving delay lines,

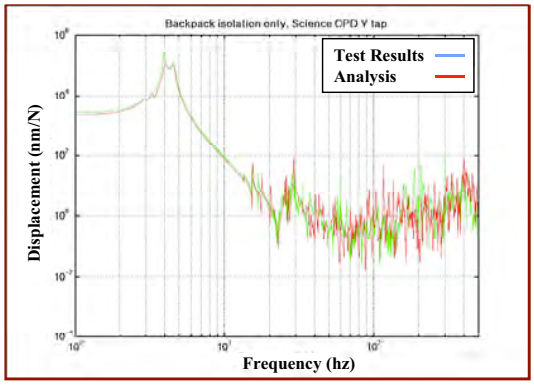

Fig. 19: STB-3 transfer function from shaker input to optical path difference output (model predict vs. test result)

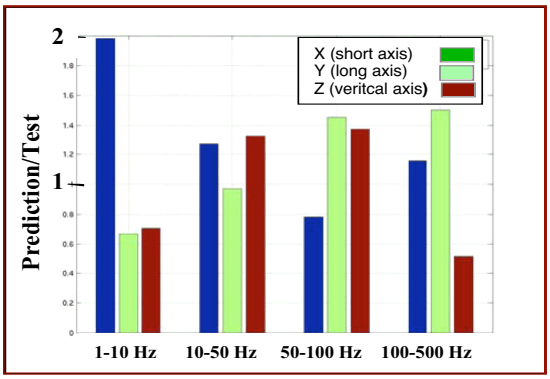

Fig. 20: STB-3 modeling uncertainty factor (MUF's) for optical path difference response, binned by frequency

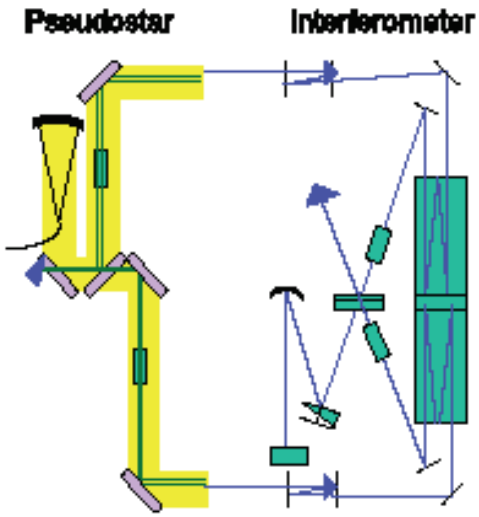

Fig. 21: Schematic of MAM interferometer and pseudostar.

surface figure errors in the interferometer optics, and fringe estimation errors. Both the MAM interferometer and IIPS were placed in a vibration-isolated, thermally stabilized vacuum chamber large enough to accommodate the 2-meter scale interferometric baselines. Doing so eliminated optical path errors due to fluctuations in the refractive index of air.

Fig. 22: MAM inverse interferometer pseudostar (IIPS) in final assembly

As is the case for SIM, MAM was operated over two different angular fields using two different observing modes. In wide angle mode, MAM observed about 50 "stars" over a 15^{o} field and did so over about one hour of observation time, proceeding from one target star to the next. In narrow angle mode, MAM observed five stars over a 1^{o} field, chopping repeatedly between them over a 15-minute time period.

The MAM performance metric is expressed in picometers of agreement between the metrology readout and the observed white light fringe position. The narrow angle metric consistent with 1 microarcsecond performance on SIM is 24 picometers. Prior to making a set of narrow angle observations data was taken to establish the noise floor of the MAM instrument. This data is also representative of the performance of SIM's guide interferometers since the guide interferometers always observe guide stars at a given, unvarying, field angle. This noise floor data, termed field independent data, was processed via the same chopping algorithm as was subsequently applied to the field dependent data. Fig. 23 shows some of our best MAM narrow angle field independent data. Note that after 10 chops, which is a lower bound for SIM observations, this data set achieves 10 picometers noise floor (the distinction between the raw data and the metric has to do with the way the data is taken and the fact that the noise reflects not only errors in the MAM instrument, which is traceable to SIM, but also errors in the IIPS, which is not SIM traceable). With a noise floor this small there was some room left for field dependent errors while still meeting the 24 picometer narrow angle metric. And indeed MAM was able to meet this metric as depicted in Fig. 24. The figure displays the performance of 20 independent ten chop narrow angle field dependent data sets taken over a one-week period in September 2003. The average of 20.2 picometers handily beat the goal level requirement and accomplished the completion of Technology Gate 6. Technology Gate 3 was achieved with an earlier data set that delivered an intermediate level of narrow angle performance.

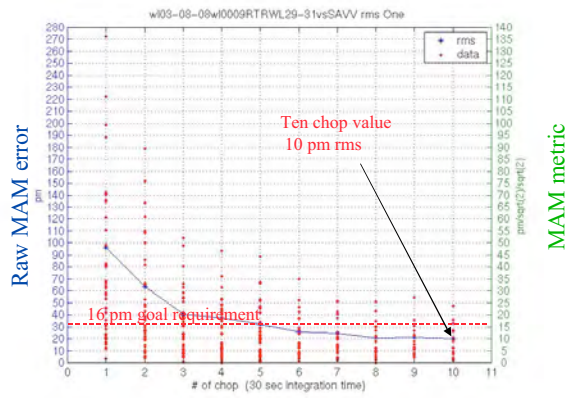

Fig 23: MAM narrow angle field independent data vs number of chops

Fig. 24: Field dependent metric summary plot for 20 narrow angle data sets

Technology Gates 5 and 7 required MAM to reach specific performance plateaus over the wide angle field of regard. Although the performance levels were considerably relaxed compared to the narrow angle field, the fact of the 15-fold

wider field and the longer time period over which data was acquired made the wide angle Gates somewhat harder to achieve. Gate 5, requiring an intermediate level of performance, was accomplished without much ado, but Gate 7 proved very challenging. Figure 25 shows a typical map of the MAM wide angle residual error from spring of 2004. Many data runs were taken and the statistical average during that period was about 400 pm, somewhat better than the Figure 25 result, but still short of the Gate 7 goal of 280 pm. However, given the fact that sufficient margin existed in the SIM astrometric error budget to absorb this performance shortfall while still meeting overall science goals, the 400 pm wide angle error was judged acceptable and Gate 7 was passed. The project's review boards did, however, impose a "lien" on Gate 7 approval. The project was tasked with explaining the distinctly asymmetric feature on the right side of the residual map of Figure 25. This feature, which came to be called "the MAM bump," was evident with great repeatability in all the data taken in spring 2004. The concern of the review boards was that some subtle phenomenology could be responsible for the bump and that this phenomenology could manifest itself with a much larger error on the full scale SIM flight instrument than was observed in the sub-scale MAM testbed. This is where our modeling team came to the rescue. After many months of experimental "bump hunting," mostly centering on testbed realignment, the modelers hit upon a theory that the bump was due to diffraction off a "spider" supporting a mask in the testbed optical path. As the testbed took data over the wide angle field, the "spider" had to rotate in the starlight beam by a few degrees. Diffraction modeling produced analytical residual maps that had a pronounced similarity to the MAM bump of Figure 25. A decision was made for the testbed team to remove the "spider" and support the mask in an alternative way. The result was the experimental residual map of Figure 26 – NO MORE MAM BUMP. Coincidentally, removal of the bump brought the RMS residual down to 280 pm, the original Technology Gate 7 goal. There certainly could not have been a more satisfying way to validate our diffraction modeling capability.

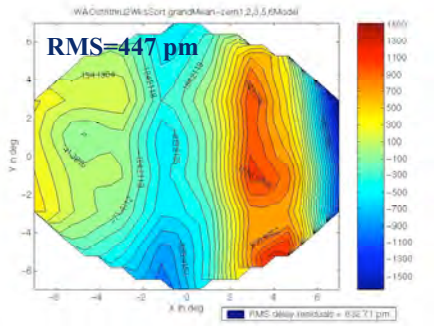

Fig. 25: Tech Gate 7 error residual over MAM wide angle field of regard

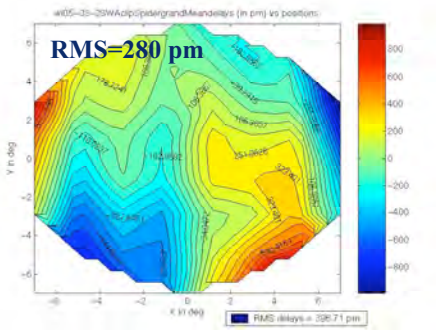

Fig. 26: MAM wide angle residual after removal of the MAM "bump"

Kite Testbed—Kite was aimed at demonstrating that the laser metrology gauges discussed above can be built up into multiple gauge configurations capable of measuring the relative motion of optical fiducials (viz., corner cubes) in more than one dimension. Such a multiple gauge configuration is referred to as an "optical truss," and the demonstration of a picometer regime optical truss was the objective of Technology Gate 4. On SIM, a three dimensional optical truss consisting of 14 gauges is used to monitor the relative motion of the corner cubes located on the system's main starlight receiving optics. The testbed that was built to demonstrate the optical truss concept is called Kite for reasons that become obvious when one looks at the configuration depicted in Fig. 27. Kite consists of 6 laser gauges in a plane originally laid out to resemble a kite. The call outs in the figure are the passive corner cube (PCC), the active corner cube (ACC), two triple corner cubes (TCC) and 6 so-called "quick prototype" or QP beam launchers of the type pictured in Fig. 5 above. Similar to MAM, the primary experiments were to articulate the ACC in tip/tilt over both the narrow and wide angle fields (±0.5˚ and ±7.5˚ respectively) and to measure any change in the geometry of the 6-gauge optical truss to about the 10 pm level for narrow angle mode and the 100 pm level for wide angle mode. Six gauges in a plane is the smallest number of gauges that allow for a multi-dimensional consistency test. That is to say, the outputs of any of five gauges is sufficient to predict the output of the sixth gauge. Agreement in these quantities to 8 pm for narrow angle and 140 pm for wide angle were the goals established for the optical truss technology consistent with SIM's astrometric science goals.

Kite attained operational status in 2002 and is shown installed in its vacuum chamber (Fig. 28). It achieved its performance goals of 8 pm on the narrow angle metric and 140 pm on the wide angle metric in early 2004 (having attained the intermediate performance levels necessary for satisfaction of Technology Gate 4 a year and a half earlier).

Typical raw data is depicted in Fig. 29, which shows the optical path length outputs of the 6 laser gauges during a long duration field independent run. Note that even without commanding any corner cube motion, the gauges sensed motions on the order of 0.2 micron as the experiment responded to temperature variations in the chamber. When the testbed consistency metric was computed, the result was the time trace in Fig. 30. Note that even though the corner cubes were drifting on the order of 200 nanometers (Fig. 29), the Kite optical truss was able to make real-time measurements of this motion that are good to under 1 nanometer RMS. And, once this "raw" metric data was processed in a SIM-like manner using thirty-second chops, the performance was in the 20 pm per chop regime as shown in Fig. 31. Once 10-chop averages were computed, the result was under 5 pm of field independent narrow angle performance. When this experiment was repeated with the ACC rotating over the narrow angle field, 10-chop performance was still maintained at the 8 pm level implying that field dependent errors were very small over the narrow angle field.

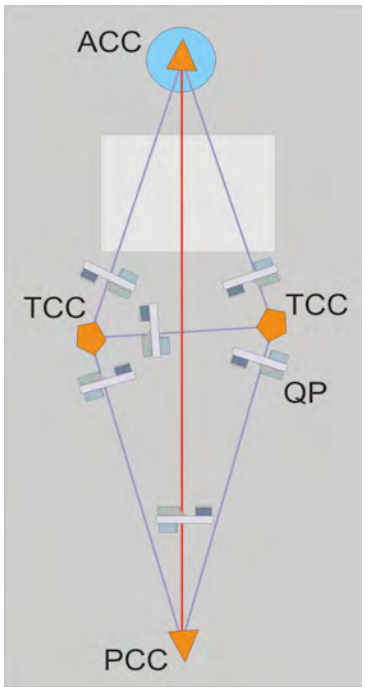

Fig. 27: Kite layout.

Wide angle performance is much more heavily field dependent than is narrow angle. The left hand plot in Fig. 32 shows a contour map of the raw Kite metric as a function of tip and tilt over the wide angle field (note that a factor of two exists between the rotation of the corner cube and rotation on the sky, implying that ±3.75˚ corner cube rotation maps to ±7.5˚ on the sky). Peak-to-peak metric errors on the order of 8 nm are seen in the figure. These are due to effects such as dihedral errors in the corner cube and bias in metrology phase as a function of corner cube incidence angle. However, these effects are dominated by low order errors over the field, which are automatically removed in SIM's science data processing. With this data processing applied performance well below the goal of 140 pm, RMS was achieved. It is also of note that these field dependent effects can be very accurately modeled, as shown in the right hand plot of Fig. 32. The plot indicates model agreement over the field of better than 6% at the worst case point. This is an extremely strong validation of our modeling techniques giving us great confidence in our flight models. Given the fact that SIM's optical truss geometry and size differ from Kite's, it is important that this modeling capability be as strong as it is.

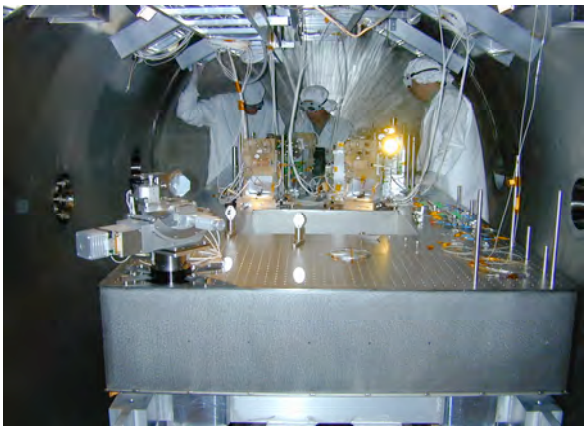
Fig. 28: Kite testbed in vacuum chamber.

Thermal Optomechanical (TOM) Testbed—TOM was aimed at exploring the response of optical figure to small changes in thermal conditions. This is a critical area for SIM. Since the SIM metrology system samples only a small portion of each collecting aperture, sub-nanometer changes to optical figure across the apertures during the course of an observation would result in misleading estimates of the optical path excursions seen by starlight. SIM's design solution is to maintain very tight (< 10 mK) thermal control of time varying gradients across the collecting optics. Thermal-optical-mechanical modeling of the flight instrument indicates that these small mirror temperature excursions will insure acceptably small distortions in optical figure. The TOM testbed's job was to prove that this is, in fact, the case.

TOM proceeded in two major steps. Step 1 was aimed at validating the ability to measure as well as model temperature changes in the single digit millikelvin regime. This was accomplished by LM ATC in an early thermal-only experiment where a 33 cm Pyrex mirror (Fig. 33) in a thermal vacuum tank was exposed to time varying thermal

loads and its temperature response recorded. These data were compared to predictive thermal models. The thermal

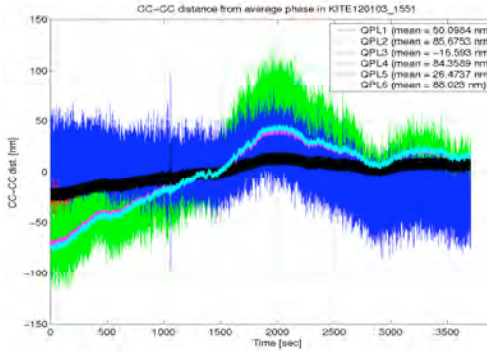

Fig. 29: Raw 6-gauge output

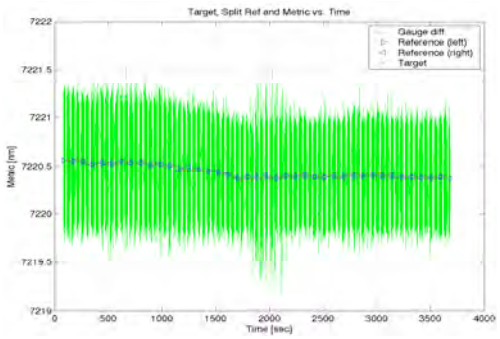

Fig. 30: Kite metric output

modeling predicted temporal changes in through-mirror temperature gradients to an accuracy of about 20% (Fig. 34). This was critical to SIM since it is the through-mirror gradients that are expected to produce the majority of mirror deformation. Having established the ability to make sufficiently accurate temperature predictions, the second major step for TOM was to demonstrate that acceptably small deformations result in flight-like optics when they are subjected to the expected SIM thermal environment. This was a major undertaking which required: (i) the fabrication of the 35-cm flight-traceable optics pictured in Figures 8 and 9; (ii) the placement of these optics in a thermal vacuum chamber where SIM flight thermal conditions were simulated; (iii) the measurement of millikelvin and picometer temperature and deformational excursions of the optics, and; (iv) the correlation of the temperature and deformation data to thermal, optical and mechanical models. These tasks were successfully accomplished, beginning with the design of the brassboard compressor and siderostat in 2003 and culminating in the 2005 thermal vacuum testing and model validation activities.

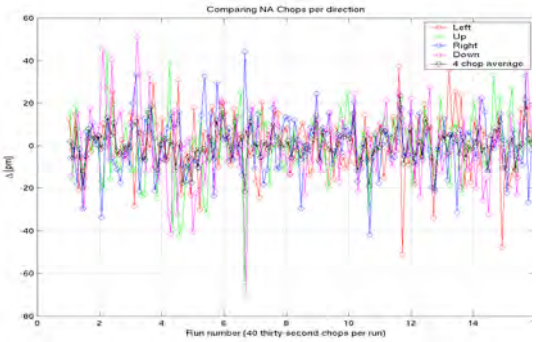

Fig. 31: Kite field independent performance with single chop narrow angle processing

A schematic of the test configuration is shown in Figure 35. All of the equipment was mounted on a large optical table inside an 11-foot diameter vacuum chamber. COPHI, which stands for Common Path Heterodyne Interferometer, is a sensor that measures picometer regime deformation of the optics. Based upon the same technology behind the picometer

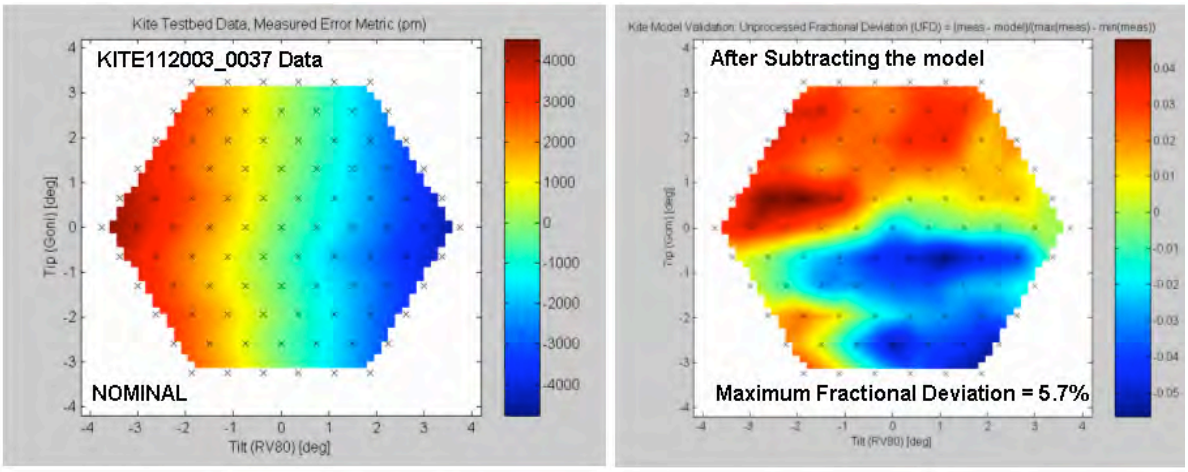

Fig. 32: Kite wide angle field dependent error (left) and modeling accuracy of same (right)

metrology beam launcher discussed earlier, COPHI sampled optical path length changes through the system at over 40 locations within the aperture. The brassboard compressor telescope (see Fig. 8 above) expanded the COPHI sensing beam to 35 cm and transferred it to the reference flat and then on to the brassboard siderostat (see Fig. 9 above) where it was retro-reflected back through the system and to COPHI's detectors and phase meter electronics. The brassboard siderostat was surrounded by a shroud where the walls could be flooded with liquid nitrogen. The walls of the shroud also contained heaters. The purpose of the shroud was to simulate the flight thermal environment for the siderostat. When cooled to the temperature of liquid nitrogen, the shroud simulated the siderostat's view of the walls of the SIM Collector Bay. The heaters were employed to change the shroud wall temperature profile to mimic the way SIM's Collector Bay walls will respond in flight as the spacecraft changes attitude with respect to the Sun. Thus, the primary TOM experiment was to make picometer level measurements of the deformation of the flight-like siderostat as it experienced flight-traceable temperature swings. Numerous millikelvin-capable thermometers were located throughout the testbed to provide temperature maps of the shroud and optics and support the thermal and optomechanical model validation effort. The purpose of the reference flat was to chop out deformations of the beam compressor (which was not thermally controlled and, hence, expected to experience relatively large deformations) in order to isolate on the distortion of the siderostat. By a stroke of luck, the naturally occurring diurnal temperature variations of the compressor did an excellent job of simulating the temperature excursions expected to occur on the compressor in flight. Thus, we were able to expand the scope of the test to include the compressor as well as the siderostat. We could turn the reference flat into retro position and measure the deformations of the compressor alone. We could chop the reference flat and measure the deformations of the siderostat alone. Or we could position the reference flat as show in Figure 35 and measure the deformations of the compressor/siderostat system, capturing the total errors that would arise in the large optics of SIM's science interferometer.

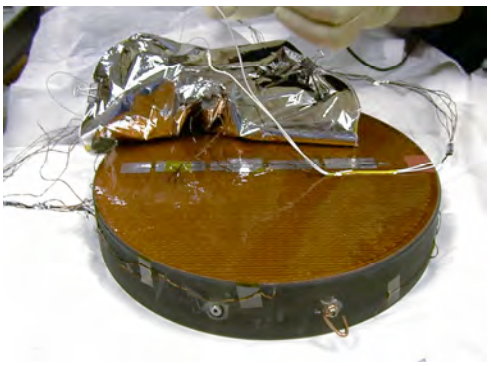

Fig. 33: Pyrex mirror for TOM test #1

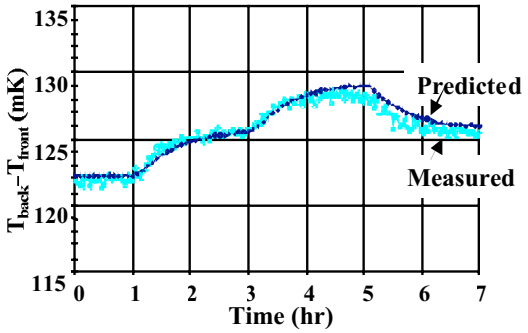

Fig. 34: Time variation of TOM mirror front-to-back thermal gradient-actual vs. predict

Typical temperature and deformation data taken from a compressor-only test are shown in Figure 36. During a 60-hour run, temperatures from five thermometers located at different positions on the compressor are seen to swing through about 0.5 degree Kelvin over each 24-hour period. Superimposed on the plot (the noisier looking trace) is the optical path difference (OPD) metric measured by COPHI. The metric is computed by taking the difference between the COPHI detector in the center of the aperture and the average of the outer annulus of COPHI detectors near the periphery of the aperture. The metric represents the optical path error between what SIM's internal metrology will measure (central detector) and the path traveled by starlight through SIM's optical beam train (average of the outer detectors). Note how closely the OPD metric tracks the temperature changes, clearly indicating a cause-and-effect relationship. The TOM testbed data enabled the modeling team to conduct an extensive model validation study. In general, it was shown that temperature changes could be predicted with high accuracy but that optical deformations were somewhat harder to model. Figure 37 is a typical comparison between

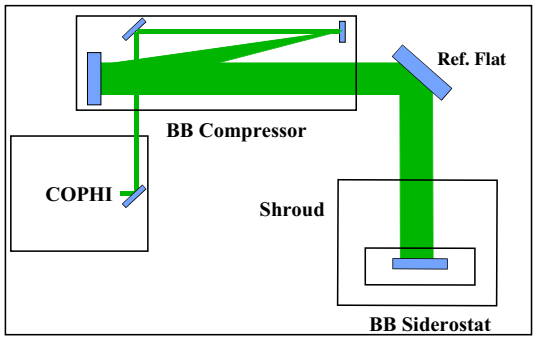

Fig. 35: TOM testbed layout

temperature predicts and temperature data. The jagged line is siderostat temperature data; each division is 20 millikelvins. The two smooth traces are model predicts, one using a priori thermal parameters and the other using an updated set of parameters that attempt to better capture the observed data. Note that both analytical curves do an excellent job of tracking the data. Note also that the model predict is quite insensitive to parameter variation. Figure 38 compares compressor deformation data, viz. the COPHI measured OPD metric, with analytical predictions of the same quantity. The analytical result is the one that displays the smallest excursion of the metric and under-predicts the experimental result by slightly less (better) than a factor of two (the other two curves, which do a better job of capturing the data, are quasi-empirical). In this case, the analytical curve is quite sensitive to changes in certain parameters, in particular the coefficient of thermal expansion (CTE) of the ULE compressor material. However, CTE values that improve the agreement are outside the factory-certified specifications, so we have used the manufacturer-supplied numbers. Nevertheless, model agreement within a factor of two is considered acceptable by the project. When we apply a MUF of two to our flight predictions, we still retain considerable margin against our allocations for siderostat and compressor deformations.

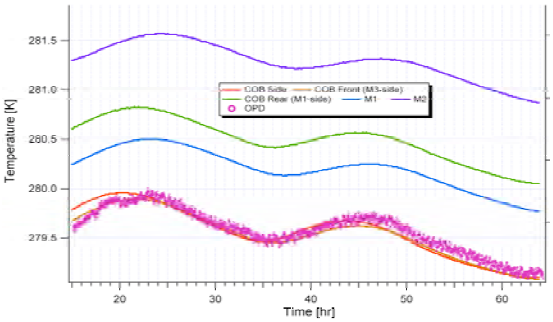

Fig. 36: Compressor temperature profile & OPD metric

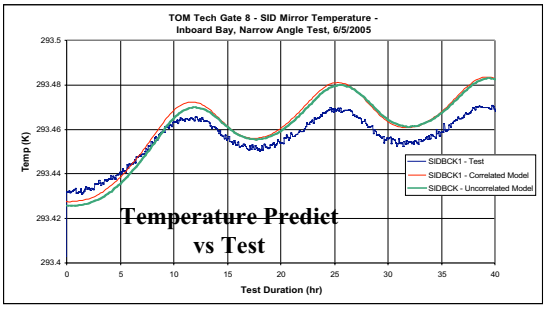

Fig. 37: Siderostat temperature measurement vs. predictions

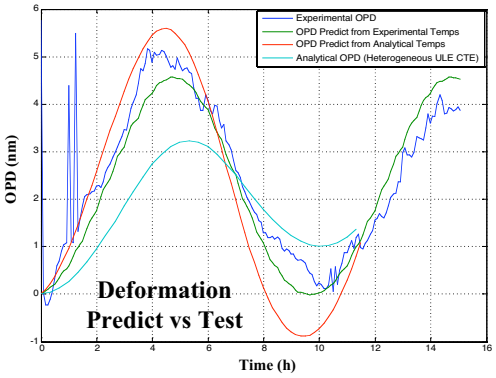

Fig. 38: Compressor deformation measurements vs. predictions

3.3 Technology Gate 8

Technology Gate 8 represented the culmination of the technology program. Its aim was to combine the performance of all of the testbeds and map them into a single system level metric to be compared against SIM's science requirements. As stated in the Technology Plan, Technology Gate 8 reads:

"Benchmark system-level instrument picometer performance against the following:

1. *wide angle*
   a. *5811 pm consistent with the SIM minimum performance level of 30 μas*
   b. *1914 pm consistent with the SIM baseline performance level of 10 μas*
   c. *704 pm consistent with the SIM goal performance level of 4 μas*
2. *narrow angle*
   a. *131 pm consistent with the SIM baseline performance level of 3 μas*
   b. *47 pm consistent with the SIM goal performance level of 1 μas*

This benchmark is to be done using a specific combination of experimental results and analysis, identifying model and test uncertainties and error budget margins. As a result of the performance level achieved, NASA will decide whether to

continue further activity to improve performance or to stop and accept the present level of activity. The completion of this milestone will demonstrate, at a system level, that SIM will meet its required instrument performance."

The block diagram of Figure 39 shows the way in which the testbed data was processed to produce mission performance predictions. At the heart of the scheme is the Instrument Model, which takes the testbed data as inputs and produces a simulated science data stream, which is then post-processed as the SIM science data will be. Since each testbed was designed to emulate a major instrument subsystem, the mapping into the blocks of the Instrument Model is rather straightforward. Kite feeds data into the model of the "external metrology sensor" and MAM (representing an interferometer "back-end") and TOM (representing an interferometer "front-end") feed data into the guide and science interferometer sensor models. The "roll sensor" block of the Instrument Model accounts for misalignments between the guide and science interferometer (as monitored by the external metrology sensor). The Instrument Model is a far more detailed and nuanced construct than an error budget. It is not constrained to combine errors under the assumption that they are statistically independent and uncorrelated. However, since its output is a time series, the Instrument Model must be run many times in order to produce statistically meaningful results.

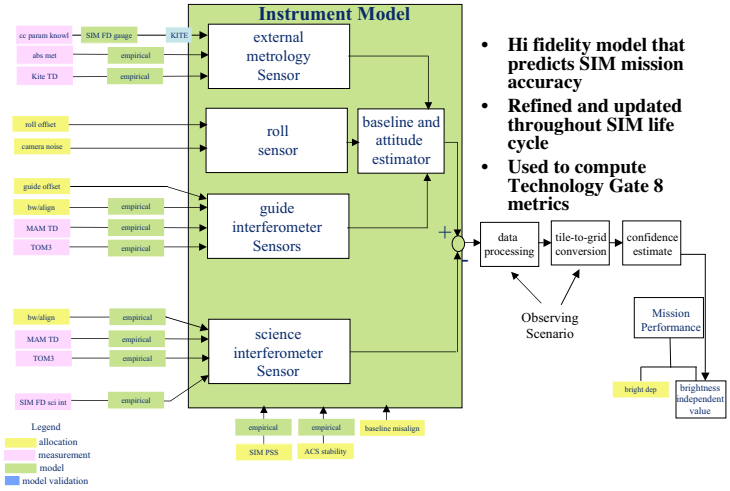

Fig. 39: Instrument Model

It is important to note that one underlying assumption of the Instrument Model is that the external metrology sensor and the interferometer sensors operate independently and don't interfere with one another. As part of the Technology Gate 8 effort, two experiments were dedicated to proving the validity of this assumption. The only places where the external metrology and interferometer sensors physically intersect are at the corner cube fiducials. Hence, the two "separability" experiments involved corner cubes and investigated their potential to cause interaction between the major sensors. One way that interaction could occur would be for stray laser light from the external metrology sensor to find its way into the metrology optics of one of the interferometers (or vice versa). This concern was laid to rest with an "optical cross-talk experiment" which showed that this effect would lead to less than a single picometer of error on SIM. The other possible source for interference arises from the fact that SIM's corner cubes have multiple faces and the external metrology sometimes samples a different face than does an interferometer's internal metrology. This could lead to disagreement between the two measurements as to the true location of the corner cube vertex. This Non-Common Vertex Error was thoroughly investigated in a sophisticated experiment that proved that this error source could be dependably calibrated. And the calibration was then independently verified in the Kite testbed.

The Instrument Model was constructed in 2004 and numerous "sanity check" cases were run on it before real testbed data was input. During the spring of 2005, Monte Carlo production runs commenced and an extensive set of statistics compiled. By June of 2005, the two Technology Gate 8 metrics, one for narrow angle astrometry and the other for wide angle, had been computed. Narrow angle came in at 1.05 microarcseconds and wide angle at 4.10 microarcseconds. Both were extremely close to goal level science performance and handily beat the baseline and minimum requirements. In July of 2005, the SIMTAC and EIRB both recommended closure of Technology Gate 8, and by the end of that month, NASA HQ had agreed.

The Instrument Model will live on and see on-going use as one of the most important products of the technology program. It will be continually refined and updated, and its predictions will serve as the official project performance estimates. During the flight system design phase, the Instrument Model will use component and subsystem level

analytical results as inputs (rather than technology testbed data). As the flight instrument is built, the input data sets will be generated initially from component testing and, ultimately, from subsystem and system level tests. These final input data sets from instrument subsystem and system tests will look remarkably like the testbed data sets that were processed in the service of Technology Gate 8.

4. TRANSITION TO FLIGHT

As the technology development effort entered its final phase over the past couple years, the SIM Project has been building its flight engineering staff and focusing increasingly on the design of the flight system. At this point, it is crucial that technology completion meshes smoothly with the flight build up otherwise the project is at risk of wasting some of the knowledge gained during the technology program. Relearning this knowledge during development of the flight instrument would be a very expensive proposition.

There are several concrete steps that the project has taken to ensure a smooth transition from technology development to flight development. First and foremost was the decision to retain the project's key technologists and place them in appropriate positions on the flight side. In general, this has been done by matching a technologist with an experienced flight manager and giving them shared responsibility for delivering flight hardware.

Another key means of accomplishing technology transfer has been via the build of brassboard hardware. Brassboards are flight-traceable hardware components that are built to the best knowledge of flight requirements at the time they are commissioned. They differ from engineering models only in the degree of paperwork that accompany them and in the maturity of requirements they are built to. Brassboards have not been built for all SIM components but only those with residual risk remaining beyond the breadboards of the technology development phase. As detailed above, these include: a 35 cm aperture compressor telescope, a 40 cm siderostat steering mirror, a double corner cube fiducial, metrology beam launchers for both the internal and external metrology systems, and components of a metrology laser source.

Finally, the area of mathematical modeling plays a special role in the transition to flight. Modeling of the SIM flight instrument is one of the cornerstones of the flight verification plan. A means of gaining confidence in the flight models is to validate the modeling techniques by applying them to predicting performance of the technology testbeds. This has been done with great success over the past several years.

5. SUMMARY

Scientifically, SIM will open new vistas, including the discovery of Earth-mass planets in our galactic neighborhood. However, from the perspective of the mid-1990s, the technology necessary to make SIM a reality looked close to impossible to achieve. Unprecedented challenges in the fields of nanometer stabilization, picometer sensing, and complex system integration and test all presented themselves. Ten years later, all of these obstacles have been overcome, and SIM PlanetQuest technology is now in place. The feasibility of measuring star positions to microarcseconds has been firmly established, and the project looks forward to applying this wonderful technology to the flight system. Indeed, the technology transfer process is already well along.

ACKNOWLEDGMENTS

The research described in this paper was carried out at the Jet Propulsion Laboratory, California Institute of Technology, under a contract with the National Aeronautics and Space Administration. The author wishes to thank Daryl Victor for help in preparing this paper. Thanks are also due to the entire JPL, Lockheed-Martin, and NGST team whose outstanding work is reported in this paper.

REFERENCES

1. R. A. Laskin and A. M. San Martin, "Control/Structure System Design of a Spaceborne Optical Interferometer," AAS/AIAA Astrodynamics Specialist Conference, August 1989.

2. S. W. Sirlin and R. A. Laskin, “Sizing of Active Piezoelectric Struts for Vibration Suppression on a Space-Based Interferometer,” Joint U.S./Japan Conference on Adaptive Structures, November 1990.
3. D. Eldred and M. O’Neal, “The Phase B Testbed Facility,” Proceedings of the ADPA Active Materials and Adaptive Structures Conference, Alexandria, VA, November 1991.
4. D. Eldred and M. O’Neal, “The JPL Phase B Interferometer Testbed,” Proceedings of 5th NASA/ DoD Control Structure Interaction Technology Conference, South Lake Tahoe, March 1992.
5. E. Anderson, M. Trudent, J. Fanson, and P. Pauls, “Testing and Application of a Viscous Passive Damper for use in Precision Truss Structures,” Proceedings of 32nd AIAA SDM Conf., pp. 2795–2807, 1991.
6. J. Fanson, G. Blackwood, and C. Chu, “Experimental Evaluation of Active-Member Control of Precision Structures,” Proceedings NASA/DOD Controls-Structure Interaction Technology 1989, NASA Conference Publication 3041, Jan 29–Feb 2, 1989.
7. J. Fanson, G. Blackwood, and C. Chu, “Active/Member Control of Precision Structures,” Proceedings of the 30th AIAA Structures, Structural Dynamics and Materials Conference, Mobile, AL, April 1989.
8. B. Wada and E. Crawley, “Adaptive Structures,” *Journal of Intelligent Material Systems and Structures*, Vol. **1**, No. 2, pp. 157–174, 1990.
9. J. Fanson, E. Anderson, and D. Rapp, “Active Structures for Use in Precision Control of Large Optical Systems,” *Optical Engineering*, Vol. **29**, No. 11, ISSN 0091-3286, pp. 1320–1327, Nov. 1990.
10. E. Anderson, D. Moore, J. Fanson, and M. Ealey, “Development of an Active Truss Element for Control of Precision Structures,” *Optical Engineering*, Vol. **29**, No. 11, ISSN 0091-3286, pp. 1333–1341, Nov. 1990.
11. C. Chu, B. Lurie, and J. O’Brien, “System Identification and Structural Control on the JPL Phase B Testbed,” Proceedings of 5th NASA/DoD Control Structure Interaction Technology Conference, South Lake Tahoe, March 1992.
12. B. Lurie, J. O’Brien, S. Sirlin, and J. Fanson, “The Dial-a-Strut Controller for Structural Damping,” ADPA/ AIAA/ASME/SPIE Conf. on Active Materials and Adaptive Structures, Alexandria VA, Nov. 5–7, 1991.
13. M. Milman and C. C. Chu, “Optimization methods for passive damper placement and tuning,” *J. Guidance, Control, and Dynamics*, to appear.
14. C. C. Chu and M. Milman, “Eigenvalue error analysis of viscously damped structures using a Ritz reduction method,” *AIAA J.*, **30**, 1992.
15. J. Fanson and M. Ealey, “Articulating Fold Mirror for the Wide Field/Planetary Camera-2,” Active and Adaptive Optical Components and Systems-2, *SPIE*, Vol. 1920, Albuquerque, 1993.
16. J. Spanos, Z. Rahman, and A. von Flotow, “Active Vibration Isolation on an Experimental Flexible Structure,” Smart Structures and Intelligent Systems, *SPIE*, 1917-60, Albuquerque, NM, 1993.
17. J. Spanos and M. O’Neal, “Nanometer Level Optical Control on the JPL Phase B Testbed,” ADPA/AIAA/ ASME/SPIE Conf. on Active Materials and Adaptive Structures, Alexandria VA, Nov. 5–7, 1991.
18. J. Spanos and Z. Rahman, “Optical Pathlength Control on the JPL Phase B Testbed,” Proceedings of 5th NASA/DoD Control Structure Interaction Technology Conference, South Lake Tahoe, March 1992.
19. J. T. Spanos, Z. Rahman, C. Chu, and J. O’Brien, “Control Structure Interaction in Long Baseline Space Interferometers,” 12th IFAC Symposium on Automatic Control in Aerospace, Ottobrunn, Germany, Sept. 7–11, 1992.
20. D. Redding and W. Breckenridge, “Optical modeling for dynamics and control analysis,” *J. Guidance, Control, and Dynamics*, **14**, 1991.
21. D. Redding, B. M. Levine, J. W. Yu, and J. K. Wallace, “A hybrid ray trace and diffraction propagation code for analysis of optical systems,” SPIE OELAse Conf., Los Angeles, CA, 1992.
22. H. C. Briggs, “Integrated modeling and design of advanced optical systems,” 1992 Aerospace Design Conf., Irvine, CA, 1992.
23. M. Milman, M. Salama, R. Scheid, and J. S. Gibson, “Combined control-structural optimization,” *Computational Mechanics*, **8**, 1991.
24. M. Milman, M. Salama, M. Wette, and C. C. Chu, “Design optimization of the JPL Phase B testbed,” 5th NASA/DoD Controls-Structures Inter-action Technology Conf., Lake Tahoe, NV, 1992.
25. M. Milman and L. Needels, “Modeling and optimization of a segmented reflector telescope,” SPIE Conf. on Smart Structures and Intelligent Materials, Albuquerque, NM, 1993.
26. L. Needels, B. Levine, and M. Milman, “Limits on Adaptive Optics Systems for Lightweight Space Telescopes,” SPIE Conf. on Smart Structures and Intelligent Materials, Albuquerque, NM, 1993.

27. G. W. Neat, L. F. Sword, B. E. Hines, and R. J. Calvet, "Micro-Precision Interferometer Testbed: End-to-End System Integration of Control Structure Interaction Technologies," Proceedings of the SPIE Symposium on OE/Aerospace, Science and Sensing, Conference on Spaceborne Interferometry, Orlando, FL, 1993.
28. L. F. Sword and T. G. Carne, "Design and Fabrication of Precision Truss Structures: Application to the Micro-Precision Interferometer Testbed," Proceedings of the SPIE Symposium on OE/Aerospace, Science and Sensing, Conference on Spaceborne Interferometry, Orlando, FL, 1993.
29. B. E. Hines, "Optical Design Issues for the MPI Testbed for Space-Based Interferometry," Proceedings of the SPIE Symposium on OE/Aerospace, Science and Sensing, Conference on Spaceborne Interferometry, Orlando, FL, 1993.
30. M. Shao, M. M. Colavita, B. E. Hines, D. H. Staelin, D. J. Hutter, K. J. Johnson, D. Mozurkewich, R. S. Simon, J. L. Hersey, J. A. Hughes, and G. H. Kaplan, "Mark III Stellar Interferometer," *Astron. Astrophysics,* **193**, pp. 357–371, 1988.
31. G. Neat, R. Laskin, J. Regner, and A. von Flotow, "Advanced Isolation/Precision Pointing Platform Testbed for Future Spacecraft Missions," 17th AAS Guidance and Control Conference, Keystone, CO, Feb. 1994.
32. M. M. Colavita, J. K. Wallace, B. E. Hines, U. Gursel, F. Malbet, D. L. Palmer, X. P. Pan, M. Shao, J. W. Yu, A. F. Boden, P. J. Dumont, J. Gubler, D. C. Koresko, S. R. Kulkarni, B. F. Lane, D. W. Mobley, and G. T. van Belle, "The Palomar Testbed Interferometer," *ApJ*, 510, 1999 (in press).
33. M. Levine, "The Interferometry Technology Program Flight Experiments: IPEX I & II," Proc. of SPIE Astronomical Telescopes and Instrumentation Conference, Kona, HI, March 1998.
34. M. Levine, R. Bruno, and H. Gutierrez, "Interferometry Program Flight Experiment #1: Objectives and Results," Proc. of 15th International Modal Analysis Conference, Santa Barbara, CA, Feb. 1998.
35. G. Blackwood, "The New Millennium Deep Space 3 Separated Spacecraft Interferometer Mission," SPIE International Symposium on Astronomical Telescopes and Instrumentation, Paper no. 3350-83, March 1998.
36. G. W. Neat, A. Abramovici, J. W. Melody, R. J. Calvet, N. M. Nerheim, and J. F. O'Brien, "Control Technology readiness for Spaceborne Optical Interferometer Missions," The Space Microdynamics and Accurate Control Symposium, Toulouse, France, May 1997.
37. C. Bell, J. Walker, and A. Lee, "Interferometer Real Time Control for the Space Interferometry Mission," AIAA/ IEEE 17th Digital Avionics Systems Conference held in Seattle, WA, 31 October–6 November 1998.
38. H.C. Briggs, D. Eldred, R. Norton, A. Kissil, W. Ledeboer, S. Sirlin, M. Levine, J. Melody, M. Milman, and L. Needels, "Program for Analysis of a Complex Opto-Mechanical System," NASA Tech Brief, Vol. 22, No. 2, Item #171.
39. C. Papadimitriou, M. Levine, and M. Milman, "Application of a Finite Element Model Updating Methodology on the IPEX-II Structure," Proc. of 15th International Modal Analysis Conference (IMAC), Santa Barbara, CA, Feb. 1998.
40. C. Papadimitriou, M. Levine, and M. Milman, "Structural Damage Detection Using Modal Test Data," International Workshop on Structural Health Monitoring, Stanford University, Sept. 18–20, 1997.
41. C.-Y. Peng, M. Levine, and W. Tsuha, "Interferometry Program Experiment IPEX-II Pre-Flight Ground Modal Test and Model Correlation Report," Report JPL D-14809, Jet Propulsion Laboratory, California Institute of Technology, Pasadena, CA, Sept. 1997 (internal document).
42. C. Papadimitriou, M. Levine, and M. Milman, "A Methodology For Finite Element Model Updating Using Modal Data," 15th VPI Symposium on Structural Dynamics and Control, Blacksburg Virginia, June 1997.
43. M. Levine and M. Milman, "Experimental Verification of Integrated Opto-Structural Model Predictions," SMACS (Space Microdynamics and Control) Conference, Toulouse, France, May 1997.
44. M. Milman and M. Levine, "Integrated Modeling Tools for Precision Multidisciplinary Systems," SMACS (Space Microdynamics and Control) Conference, Toulouse, France, May 1997.
45. M. B. Levine, M. H. Milman, and A. Kissil, "Mode Shape Expansion Techniques for Prediction: Experimental Evaluation," *AIAA Journal*, Vol. **34**, No. 4, April 1996.
46. Y. Gursel, "Laser metrology gauges for OSI," Proceedings of SPIE conference on Spaceborne Interferometry, Vol. 1947, pp. 188–197, 1993.
47. Y. Gursel, "Metrology for spatial interferometry," Proceedings of SPIE conference on Amplitude and Intensity Spatial Interferometry, Vol. 2200, pp. 27–34, 1994.
48. Y. Gursel, "Metrology for spatial interferometry II," Proceedings of SPIE conference on Spaceborne Interferometry II, Vol. 2477, p. 240–258, 1995.
49. Y. Gursel, "Metrology for spatial interferometry III," Proceedings of SPIE conference on Space Telescopes and Instruments IV, Vol. 2807, pp. 148–161, 1996.

50. Y. Gursel, “Metrology for spatial interferometry IV,” Proceedings of SPIE conference on Small Spacecraft, Space Environments, and Instrumentation Technologies, Vol. 3116, pp. 12–26, 1997.
51. Y. Gursel, “Metrology for spatial interferometry V,” Proceedings of SPIE conference on Astronomical Interferometry, Vol. 3350, pp. 571–587, 1998.
52. S. S. Joshi, J. W. Melody, and G. W. Neat, “A Case Study on the Role of Structural/Optical Model Fidelity in Performance Prediction of Complex Opto-Mechanical Instruments,” IEEE Conference on Decision and Control San Diego, CA, December 1997.
53. S. S. Joshi, J. W. Melody, G. W. Neat, and A. Kissil, “Benefits of Model Updating: A Case Study Using the Micro-Precision Interferometer Testbed,” Proceedings of DETC’97 1997 ASME Design Engineering Technical Conference, Sacramento, CA, September 14–17, 1997.
54. S. S. Joshi, M. Milman, and J. W. Melody, “Optimal Passive Damper Placement Methodology for Interferometers Using Integrated Structures/Optics Modeling,” AIAA Guidance, Navigation, and Controls Conference, New Orleans, LA, August 1997.
55. J. Davis, W. J. Tango, A. J. Booth, T. A. ten Brummelaar, R. A. Minard, and S. M. Owens, “The Sydney University Stellar Interferometer I: The Instrument,” Accepted by Monthly Notices of the Royal Astronomical Society.
56. S. Shaklan, S. Azevedo, R. Bartos, A. Carlson, Y. Gursel, P. Halverson, A. Kuhnert, Y. Lin, R. Savedra, and E. Schmidtlin, “The micro-arcsecond metrology testbed (MAM),” Proceedings of SPIE conference on Astronomical Interferometry, Vol. 3350, pp. 571–587, 1998.
57. A. Kuhnert, S. Shaklan, Y. Gursel, S. Azevedo, and Y. Lin, “Metrology for the micro-arcsecond metrology testbed,” Proceedings of SPIE conference on Astronomical Interferometry, Vol. 3350, pp. 571–587, 1998.
58. S. Dubovitsky, D. Seidel, D. Liu, and R. Gutierrez, “Metrology source for high-resolution heterodyne interferometer laser gauges,” Proceedings of SPIE conference on Astronomical Interferometry, Vol. 3350, pp. 571–587, 1998.
59. A. Carlson, S. Shaklan, R. Bartos, and S. Azevedo, “Opto/mechanical design of the micro-arcsecond metrology testbed interferometer,” Proceedings of SPIE conference on Astronomical Interferometry, Vol. 3350, pp. 571–587, 1998.
60. E. Schmidtlin, S. Shaklan, and A. Carlson, “Novel wide field-of-view retroreflector for the Space Interferometry Mission,” Proceedings of SPIE conference on Astronomical Interferometry, Vol. 3350, pp. 571–587, 1998.
61. M. M. Colavita, A. F. Boden, S. L. Crawford, A. B. Meinel, M. Shao, P. N. Swanson, G. T. van Belle, G. Vasisht, J. M. Walker, J. K. Wallace, and P. L. Wizinowich, “Keck Interferometer,” Proc. SPIE 3350, 776–784, 1998.
62. A. F. Boden, C. D. Koresko, G. T. van Belle, M. M. Colavita, P. J. Dumont, J. Gubler, S. R. Kulkarni, B. F. Lane, D. Mobley, M. Shao, and J. K. Wallace, “The Visual Orbit of Iota Pegasi,” *ApJ*, 1998 (in press).
63. M. M. Colavita, “Fringe Visibility Estimators for the Palomar Testbed Interferometer,” *PASP*, 1999 (in press).
64. G. T. van Belle, B. F. Lane, R. R. Thompson, A. F. Boden, M. M. Colavita, P. J. Dumont, D. W. Mobley, D. Palmer, M. Shao, G. X. Vasisht, J. K. Wallace, M. J. Creech-Eakman, C. D. Koresko, S. R. Kulkarni, X. P. Pan, and J. Gubler, “Radii and Effective Temperatures for G, K and M Giants and Supergiants,” *AJ*, 1999 (in press).
65. C. D. Koresko, G. T. van Belle, A. F. Boden, M. M. Colavita, M. J. Creech-Eakman, P. J. Dumont, J. Gubler, S. R. Kulkarni, B. F. Lane, D. W. Mobley, X. P. Pan, M. Shao, and J. K. Wallace, “The Visual Orbit of the 0.002" RS CVn Binary Star TZ Triangulum from Near-Infrared Long-Baseline Interferometry,” *ApJL*, 1998 (in press).
66. F. Malbet, J.-P. Berger, M. M. Colavita, M. Shao, J. K. Wallace, A. F. Boden, G. T. van Belle, D. W. Mobley, C. Beichman, C. D. Koresko, S. R. Kulkarni, B. F. Lane, and X. P. Pan, “A Protoplanetary disk around FU Orionis Resolved by Infrared Long-Baseline Interferometry,” *ApJL*, 1998 (in press).
67. A. F. Boden, G. T. van Belle, M. M. Colavita, P. J. Dumont, J. Gubler, C. D. Koresko, S. R. Kulkarni, B. F. Lane, D. W. Mobley, M. Shao, and J. K. Wallace, “An Interferometric Search for Bright Companions to 51 Pegasi,” *ApJL*, **504** L39, 1998.
68. R. L. Grogan, G. H. Blackwood, and R. J. Calvet, “Optical Delay Line Nanometer Level Pathlength Control Law Design For Space-Based Interferometry,” Proceedings of the 1998 SPIE International Symposium on Astronomical Telescopes and Instrumentation Astronomical Interferometry, April 1998.
69. R. L. Grogan and R. Laskin, “On Multidisciplinary Modeling of the Space Interferometry Mission,” Proceedings of the 1998 American Controls Conference, June 1998.
70. R. J. Calvet, B. Joffe, D. Moore, R. L. Grogan, and G. H. Blackwood, “Enabling Design Concepts for a Flight-Qualifiable Optical Delay Line,” Proceedings of the 1998 SPIE International Symposium on Astronomical Telescopes and Instrumentation Astronomical Interferometry, April 1998.
71. P. B. Kahn and J. Yu, “Space Interferometry Mission: New System Engineering Approaches, Tools, Models and Testbeds,” 1998 IEEE Aerospace Conference, March 1998.

72. P. B. Kahn, “Space Interferometry Mission: A Systems Perspective,” 2000 IEEE Aerospace Conference, March 2000.
73. K. Aaron, D. Stubbs, and K. Kroenig, “Space Interferometry Mission (SIM) Instrument Mechanical Layout,” 2000 IEEE Aerospace Conference, March 2000.
74. F. Zhao, R. T. Diaz, P. Dumont, P. G. Halverson, S. Shaklan, R. E. Spero, L. Ames, S. Barrett, R. Barrett, R. Bell, R. Benson, G. Cross, K. Dutta, T. Kvamme, B. Holmes, D. Leary, P. Perkins, M. Scott, and D. Stubbs, “Development of Sub-nanometer Racetrack Laser Metrology for External Triangulation Measurement for the Space Interferometry Mission,” American Society of Precision Engineering Annual Meeting, Arlington, VA, November 10–15, 2001.
75. P. G. Halverson, F. Zhao, R. Spero, S. Shaklan, O. P. Lay, S. Dubovitsky, R. T. Diaz, R. Bell, L. Ames, and K. Dutta, “Techniques for the Reduction of Cyclic Errors in Laser Metrology Gauges for the Space Interferometry Mission,” American Society of Precision Engineering Annual Meeting, Arlington, VA, November 10–15, 2001.
76. F. Zhao, “Demonstration of Sub-Angstrom Cyclic Nonlinearity using Wavefront-division Sampling with a Common-path Laser Heterodyne Interferometer,” American Society of Precision Engineering Annual Meeting, Arlington, VA, November 10–15, 2001.
77. F. Zhao, R. T. Diaz, P. G. Halverson, G. M. Kuan, and S. Shaklan, “Wavefront versus amplitude division high precision displacement measuring interferometers,” Proceedings of Optoelectronic Distance/Displacement Measurements and Applications (ODIMAP II), Pavia, Italy, September 20–22, 2001.
78. P. G. Halverson, L. S. Azevedo, R. T. Diaz, and R. E. Spero, “Characterization of picometer repeatability displacement metrology gauges,” Proceedings of Optoelectronic Distance/Displacement Measurements and Applications (ODIMAP II), Pavia, Italy, September 20–22, 2001.
79. S. Shaklan, T. J. Shen, M. H. Milman, and A. C. Kuhnert, “Picometer measurement of white-light interference fringes,” Proceedings of Optoelectronic Distance/Displacement Measurements and Applications (ODIMAP II), Pavia, Italy, September 20–22, 2001.
80. A. C. Kuhnert, S. B. Shaklan, J. Shen, A. Carlson, and L. S. Azevedo, “First tests of the interferometer in the micro-arcsecond metrology testbed (MAM),” Proc. SPIE Vol. 4006, pp. 815–827, Interferometry in Optical Astronomy, (2000).
81. P. G. Halverson, A. Kuhnert, J. Logan, M. Regher, S. Shaklan, R. Spero, F. Zhao, T. Chang, R. Gutierrez, E. Schmitdlin, T. Vanzandt, and J. Yu, “Progress toward picometer accuracy laser metrology for the Space Interferometry Mission,” Proceedings of the International Conference for Space Optics (ICSO), Toulouse, France, December 5–7, 2000.
82. F. Zhao, J. E. Logan, S. Shaklan, and M. Shao, “A common-path, multi-channel heterodyne laser interferometer for sub-nanometer surface metrology,” International Conference on Optical Engineering for Sensing and Nanotechnology (ICOSN’99), Proc. SPIE Vol. 3740 (1999).
83. P. G. Halverson, D. R. Johnson, A. Kuhnert, S. B. Shaklan, and R. Spero, “A Multichannel Averaging Phasemeter for Picometer Precision Laser Metrology,” International Conference on Optical Engineering for Sensing and Nanotechnology (ICOSN’99), Proc. SPIE Vol. 3740 (1999).
84. Y. Lin, R. D. Bartos, R. P. Korechoff, and S. B. Shaklan, “Space beam combiner for long-baseline interferometry,” Proc. SPIE Vol. 3649, p. 134–143, Sensors, Cameras, and Systems for Scientific/Industrial Applications, (1999).
85. H. Drosdat, “Integration and Test Challengesfor the Space Interferometry Mission (SIM) Flight System,” Wavefront Controls Conference, November 14, 2000.
86. P. C. Irwin and R. Goullioud, “Hardware Design and Object-Oriented Hardware Driver Design for the Real-Time Interferometer Control Systems Testbeds,” SPIE’s Int. Sym. On Astronomical Telescopes and Instrumentation, vol. 3350, March 1998.
87. J. F. O’Brien, R. Goullioud, and G. W. Neat, “Microprecision Interferometer: Evaluation of New Disturbance Isolation Solutions,” SPIE’s Int. Sym. on Smart Structures and Materials, vol. 3327, March 1998.
88. R. Goullioud, F. G. Dekens, and G. W. Neat, “Micro-Precision Interferometer: Scorecard on Technology Readiness for the Space Interferometer Mission,” Proc. of SPIE Conference on Interferometry in Optical Astronomy, vol. 4006, March 2000.
89. R. Goullioud and A. Azizi, “Optical Design of the SIM System Testbed 3,” Proc. of SPIE Conference on Interferometry in Optical Astronomy, vol. 4006, March 2000.
90. J. H. Ambrose, A. Hashemi, J. Schneider, D. Stuggs, K. Aaron, M. Shao, and T. VanZandt, “Measurement and Prediction of Temperature Distributions in Optical Elements in the MilliKelvin Regime,” 2000 International Mechanical Engineering Congress and Exhibition, Orlando, FL, November 5–10, 2000.

91. K. M. Aaron, W. H. Mateer II, and R. L. Baron, "SIM Configuration Trades," SPIE Astrometric Interferometry Conference, March 20–24, 1998.
92. R. L. Baron, M. H. Milman, and K. M. Aaron, "SIM vs. SOS: A Space Interferometry Trade Study," SPIE Astrometric Interferometry Conference, 20–24 March 1998.
93. K. M. Aaron, presented "Space Interferometry Mission Overview," Northern California SAMPE Composite Workshop, Sunnyvale, CA, January 28, 1999.
94. K. M. Aaron, "SIM Configuration Evolution," IEEE Aerospace Conference, March 6–13, 1999.
95. K. M. Aaron, D. M. Stuggs and K. Kroening, "Space Interferometry Mission Instrument Mechanical Layout," IEEE Aerospace Conference, March 18–25, 2000.
96. O. S. Alvarez-Salazar, R. Goullioud, B. Nemati, and A. Azizi, "Path feed forward performance of an astrometric 3-BL interferometer testbed (STB-3): mitigating atmospheric effects," SPIE Conference on Astronomical Telescopes: Interferometers in Space, Waikoloa, Hawaii, USA, vol. 4852, 22–28 August 2002.
97. R. Goullioud, O. S. Alvarez-Salazar, and B. Nemati, "Dim star fringe stabilization using path length feed-forward on the SIM Test-Bed 3 (STB3)," SPIE Conference on Astronomical Telescopes: Interferometers in Space, Waikoloa, Hawaii, USA, 22–28 August 2002.
98. O. S. Alvarez-Salazar and R. Goullioud, "Combined feed-forward and feedback control for dim star fringe tracking on the SIM Test-Bed 3," IEEE Aerospace Conference, Big Sky, Montana, March 2003.
99. P. G. Halverson, O. S. Alvarez-Salazar, et al., "Progress towards picometer accuracy laser metrology for the Space Interferometry Mission—Update for ICSO 2004," Proceedings of ICSO 2004, 5th International Conference on Space Optics, Toulouse, France, March 2004.
100. O. S. Alvarez-Salazar, R. Goullioud, and A. Azizi, "Space Interferometry Mission System Testbed-3: Architecture," IEEE Aerospace Conference, Big Sky, Montana, March 2004.
101. O. S. Alvarez-Salazar, R. Goullioud, and A. Azizi, "Space Interferometry Mission System Testbed-3: External Metrology Inversion," IEEE Aerospace Conference, Big Sky, Montana, March 2004.
102. O. S. Alvarez-Salazar, "SIM System Testbed: 3-baseline stellar interferometer on a 9-meter long flexible structure," SPIE Conference on Astronomical Telescopes and Instrumentation: New Frontiers in Stellar Interferometry, Glasgow, Scotland, United Kingdom, 21–25 June 2004.
103. O. S. Alvarez-Salazar, "Metrology System for Space Interferometry Mission's System Testbed 3," SPIE Conference on Astronomical Telescopes and Instrumentation: New Frontiers in Stellar Interferometry, Glasgow, Scotland United Kingdom, 21–25 June 2004.
104. M. W. Regehr, B. Hines, and B. Holmes, "Optical Path Control in the MAM Testbed," IEEE Aerospace Conference, March 8–15, 2003.
105. Y. Gursel, "Very high-precision absolute surface metrology gauges for building and qualifying SIM testbed interferometer compound optics," in Proceedings of SPIE, Interferometry in Space, Vol. 4852, pages 355–368, 2003.
106. A. J. Bronowicki and R. MacDonald–TRW Space and Electronics Group, Y. Gursel, R. Goullioud, and T. Neville–Jet Propulsion Laboratory, "Dual-Stage passive vibration isolation for optical interferometer missions," in Proceedings of SPIE, Interferometry in Space, Vol. 4852, pp. 753–763, 2003.
107. Y. Gursel and E. A. McKenney, "An attitude control system for the SIM Test Bed 3 (STB3)," in Proceedings of SPIE, Interferometry in Space, Vol. 4852, pp. 764–777, 2003.
108. Y. Gursel, "A picometer-accuracy, laser-metrology gauge for Keck Interferometer differential-phase subsystem," in Proceedings of SPIE, Interferometry for Optical Astronomy II, Vol. 4838, pp. 995–1010, 2003.
109. J. Ambrose, A. Hashemi, J. Schneider, D. Stubbs, K. Aaron, M. Shao, and T. VanZandt "Measurement and Prediction of Temperature Distributions in Optical Elements in the mK Regime," pp. 135–145, HTD-Vol. 366-5, IMECE 2000, Orlando, FL, November 2000.
110. J. S. Pecson and A. Hashemi, "Space Interferometry Mission Thermal Design," Spacecraft Thermal Control Technology Workshop, The Aerospace Corporation, El Segundo, CA, February 28–March 2, 2001.
111. J. S. Pecson and A. Hashemi, "Multidiscipline Analysis for Space Optical Systems," AIAA 2002-0358, 40th AIAA Aerospace Sciences Meeting and Exhibit, Reno, NV, 14–17 January 2002.
112. K. M. Aaron, A. Hashemi, P. Morris, "Space Interferometry Mission Thermal Design," SPIE 4852-49, Astronomical Telescopes and Instrumentation Conference, Proceedings of SPIE Vol. 4852, Waikoloa, HI, 22–28 August 2002.
113. J. Pecson, A. Hashemi, J. Ambrose, and K. Aaron "Precision Temperature Control," *Spacecraft Thermal Control Handbook*: Fundamental Technologies, David G. Gilmore (ed.), The Aerospace Corporation, Aerospace Press, ISBN. 1-884989-1 1-X, October 2002.

114. D. Pytel and A. Hashemi, "Precision Temperature Measurement and Modeling," Spacecraft Thermal Control Workshop, The Aerospace Corporation, El Segundo, CA, March 9–11, 2003.
115. J. Batson and A. Hashemi, "Precision Modular Thermal Deformation Modeling," Spacecraft Thermal Control Workshop, The Aerospace Corporation, El Segundo, CA, March 9–11, 2003.
116. D. B. Schaechter, P. E. Perkins, P. V. Mammini, D. A. Swanson, C. W. Tischhauser, R. S. Benson, T. B. Andersen, R. S. Bruner, R. I. Fowler, K. T. Morimoto, and L. A. Sievers, "Diffraction Hardware Testbed and Model Validation," SPIE Astronomical Telescopes and Instrumentation Conference, Interferometry in Space, August 2002.
117. J. E. Logan, P. G. Halverson, M. W. Regehr, and R. E. Spero, "Automatic alignment of a displacement-measuring heterodyne interferometer," *Appl Optics* 41 (**21**): 4314–4317, July 20, 2002.
118. P. G. Halverson and R. E. Spero, "Signal processing and testing of displacement metrology gauges with picometer-scale cyclic nonlinearity," *J Opt A-Pure Appl Op* 4 (**6**), S304–S310, Nov. 2002.
119. C. G. Asbury, D. T. Liu, J. L. Mulder, J. G. Hawley, A. C. Mehta, and S. Dubovitsky, "Laser-welded packaging of a Nd:YAG laser for space applications," Proceedings of SPIE's International Symposium on Astronomical Telescopes and Instrumentation, Vol. 4852, Part 2, pp. 593–601, 2002.
120. R. Korechoff and L. Sievers, "Sub-nanometer level model validation of SIM interferometer," SPIE Conference on New Frontiers in Stellar Interferometry, Glasgow, Scotland, June 2004.
121. X. Pan, R. Goullioud, J. Yu, and M. Shao, "SIM Spectral Characteristics and Accuracy Analysis," SPIE Conference on New Frontiers in Stellar Interferometry, Glasgow, Scotland, June 2004.
122. X. Pan, M. Shao, "Accuracy and Stability of fringe Measurements in SIM," ASP Conference Series (in press), 2005.
123. C. Zhai, M. Milman, and M. Regehr, "The Least-Squares Calibration on the Micro-Arcsecond Metrology Test Bed," Proceedings of the Symposium on Astronomical Telescopes and Instrumentation, Orlando, FL, 2006.
124. B. Nemati and G. Kuan, "Model Validation of SIM External Metrology at the Sub-Nanometer Level, " Proc. SPIE Int. Soc. Opt. Eng., Vols. 5491, 1823, 2004.
125. G. Kuan and S. Moser, "Sensitivity of Optical Metrology Calibration to Measured Corner Cube Retroreflector Parameters for the Space Interferometry Mission, " Proc. SPIE Int. Soc. Opt. Eng., Vols. 4852, 795, 2003.
126. G. Sun, O. S. Alvarez-Salazar, A. Azizi, "Dim Star Tracking for Stellar Interferometery," IEEE Aerospace Conference, Big Sky, Montana, March 2005.
127. R. Goullioud, B. E. Hines, C. E. Bell, T. J. Shen, E. E. Bloemhof, "SIM Astrometric Demonstration at the 150 Picometer level using the MAM Testbed, " IEEE Aerospace Conference, Big Sky, Montana, 2003.
128. M. W. Regehr, B. Hines, and B. Homes, "Optical Path Control in the MAM Testbed, " IEEE Aerospace Conference, Big Sky, Montana, 2003.
129. R. Goullioud and T. J. Shen, "SIM Astrometric Demonstration at 24 Picometers on the MAM Testbed," IEEE Aerospace Conference, Big Sky, Montana, 2004.
130. R. Goullioud and T. J. Shen, "MAM Testbed Detail Description and Alignment, " IEEE Aerospace Conference, Big Sky, Montana, 2004.
131. R. Goullioud, T. J. Shen, and J. H. Catanzarite, "Wide Angle Astrometric Demonstration on the Micro-Arcsecond Metrology Testbed for the Space Interferometry Mission, " International Conference on Space Optics, Toulouse, France, 2004.
132. R. Goullioud, T. J. Shen, and J. H. Catanzarite, "SIM Narrow and Wide Angle Astrometric Demonstration on the MAM Testbed, " SPIE Conf. on New Frontiers in Stellar Interferometry, Vol. 5491, 2004.
133. R. P. Korechoff, D. J. Hoppe, X. Wang, "Sub-nanometer Level Model Validation of the SIM Interferometer," SPIE Conf. on New Frontiers in Stellar Interferometry, Vol. 5491, 2004.
134. R. Goullioud, C. A. Lindensmith, I. Hahn, "Results from the TOM3 Testbed: Thermal Deformation of Optics at the Picometer Level, " IEEE Aerospace Conference, Big Sky, Montana, 2006.
135. C. A. Lindensmith, H. C. Briggs, Y. Beregovski, V. A. Feria, R. Goullioud, Y. Gursel, I. Hahn, G. Kinsella, M. Orzewalla, C. Phillips, "Development and Validation of High Precision Thermal, Mechanical, and Optical Models for the Space Interferometry Mission, " IEEE Aerospace Conference, Big Sky, Montana, 2006.
136. H. Tang and F. Zhao, " Estimation of Cyclic Error due to Scattering in the Internal OPD Metrology of the Space Interferometry Mission, " 8th International Symposium on Laser Metrology, Mexico, February 2005.
137. F. G. Dekens, O. S. Alvarez-Salazar, A. Azizi, S. J. Moser, B. Nemati, J. Negron, T. Neville, and D. Ryan, "Kite: Status of the External Metroogy Testbed for SIM, " Proc. SPIE Int. Soc. Opt. Eng. Vols. 5491, 1020, 2004.